STUDY OF LAMINAR FLAME 2-D SCALAR VALUES AT VARIOUS FUEL TO AIR RATIOS USING AN IMAGING FOURIER-TRANSFORM SPECTROMETER AND 2-D CFD ANALYSIS

THESIS

Andrew J. Westman, Captain, USAF

AFIT-ENP-13-M-36

DEPARTMENT OF THE AIR FORCE
AIR UNIVERSITY

AIR FORCE INSTITUTE OF TECHNOLOGY

Wright-Patterson Air Force Base, Ohio

AFIT-ENP-13-M-36

STUDY OF LAMINAR FLAME 2-D SCALAR VALUES AT VARIOUS FUEL TO AIR RATIOS USING AN IMAGING FOURIER-TRANSFORM SPECTROMETER AND 2-D CFD ANALYSIS

THESIS

Presented to the Faculty

Department of Physics

Graduate School of Engineering and Management

Air Force Institute of Technology

Air University

Air Education and Training Command

In Partial Fulfillment of the Requirements for the

Degree of Master of Science in Applied Physics

Andrew J. Westman, BS

Captain, USAF

March 2013

AFIT-ENP-13-M-36

STUDY OF LAMINAR FLAME 2-D SCALAR VALUES AT VARIOUS FUEL TO AIR RATIOS USING AN IMAGING FOURIER-TRANSFORM SPECTROMETER AND 2-D CFD ANALYSIS

Andrew J. Westman, BS
Captain, USAF

Approved:

_____	_____
Kevin C. Gross, PhD. (Chairman)	Date
_____	_____
Glen P. Perram, PhD. (Member)	Date
_____	_____
Viswanath R. Katta, PhD. (Member)	Date

Abstract

This work furthers an ongoing effort to develop imaging Fourier-transform spectrometry (IFTS) for combustion diagnostics and to validate reactive-flow computational fluid dynamics (CFD) predictions. An ideal, laminar flame produced by an ethylene-fueled (C_2H_4) Hencken burner (25.4 x 25.4 mm^2 burner) with N_2 co-flow was studied using a Telops infrared IFTS featuring an Indium Antimonide (InSb), 1.5 to 5.5 μm, focal-plane array imaging the scene through a Michelson interferometer. Flame equivalency ratios of Φ = 0.81, 0.91, and 1.11 were imaged on a 128 x 200 pixel array with a 0.48 mm per pixel spatial resolution and 0.5 cm^{-1} spectral resolution. A single-layer radiative transfer model based on the Line-by-Line Radiative Transfer Model (LBLRTM) code and High Resolution Transmission (HITRAN) spectral database for high-temperature work (HITEMP) was used to simultaneously retrieve temperature (T) and concentrations of water (H_2O) and carbon dioxide (CO_2) from individual pixel spectra between 3100-3500 cm^{-1} spanning the flame at heights of 5 mm and 10 mm above the burner. CO_2 values were not determined as reliably as H_2O due to its smooth, unstructured spectral features in this window. At 5 mm height near flame center, spectrally-estimated T's were 2150, 2200, & 2125 K for Φ = 0.81, 0.91, & 1.11 respectively, which are within 5% of previously reported experimental findings. Additionally, T & H_2O compared favorably to adiabatic flame temperatures (2175, 2300, 2385 K) and equilibrium concentrations (10.4, 11.4, 12.8 %) computed by NASA-Glenn's Chemical Equilibrium with Applications (CEA) program. UNICORN CFD predictions were in excellent agreement with CEA calculations at flame center, and

predicted a fall-off in both T and H_2O with distance from flame center more slowly than the spectrally-estimated values. This is likely a shortcoming of the homogeneous assumption imposed by the single-layer model. Pixel-to-pixel variations in T and H_2O were observed which could exceed statistical fit uncertainties by a factor of 4, but the results were highly correlated. The T x H_2O product was smooth and within 3.4 % of CEA calculations at flame center and compared well with CFD predictions across the entire flame. Poor signal-to-noise (SNR) in the calibration is identified as the likely cause of this systematic error. Developing a multi-layer model to handle flame inhomogeneities and methods to improve calibration SNR will further enhance IFTS as a valuable tool for combustion diagnostics and CFD validation.

Acknowledgments

I'd like to thank my advisor, Dr. Kevin Gross, for his patience in teaching an engineer about physics, his dedication to the work, and his much needed guidance in the creation of this document. Dr. Viswanath Katta also provided crucial components for this project. Dr. Katta's expertise and instruction on the use of computational fluid dynamics were invaluable. I'd also like to thank Dr. Glen Perram for his valuable instruction and insights into improving the subject matter of this document. Lastly, I'd like to thank God, friends, and family. Without them I'd surely have gone insane.

Andrew J. Westman

Table of Contents

Page

List of Figures

List of Tables

Page

STUDY OF LAMINAR FLAME 2-D SCALAR VALUES AT VARIOUS FUEL TO AIR RATIOS USING AN IMAGING FOURIER-TRANSFORM SPECTROMETER AND 2-D CFD ANALYSIS

I. Introduction

Motivation

Hyper-spectral remote sensing can be utilized to discern scalar values during combustion events to include temperature and species concentrations. Developing tools to increase the effectiveness and capabilities of these remote sensing methods can lead to more efficient combustion diagnostics and turbulent flow field study. Improved understanding of laminar and turbulent flow fields can in turn lead to improved computational fluid dynamics (CFD) models and combustor designs in aircraft as well as more efficient gas laser systems.

Research Topic

Imaging Fourier-Transform Spectrometers (IFTS) have been successfully demonstrated by Gross et al. [1,2] among others as a means to efficiently and passively recover spectroscopic data including species concentrations, temperature, and density. These parameters are useful in the study of various flow fields, to include: jet engine exhaust [1], smokestacks [2], near laminar burners [3], and turbulent flames to name a few. These parameters can be accurately measured using laser-based spectroscopy methods. However, tracking multiple species concentrations is difficult with lasers due to the small bandwidth nature of laser sources. Additionally, laser-based techniques often require an extensive laboratory setup [1].

The IFTS device uses a high frame rate, passive sensor with high resolution across a broad bandwidth. These qualities are particularly useful when attempting to attain flow field data outside of a laboratory [1]. Gross et al. provides an excellent example of IFTS utility by quantifying species concentrations in a non-reacting turbulent exhaust plume exiting a coal-fired power plant [2]. Another example, provided by Rhoby et al., is determining two-dimensional scalar measurements of flame properties. These flame data are useful for studying combustion phenomenon and validating/verifying chemical kinetic and numerical models [3].

Near laminar burners such as the Hencken burner are commonly used to calibrate measurement devices or validate experimental temperature measurement methods. The Hencken burner can be setup to produce a nearly steady, almost adiabatic and nearly laminar flame [4]. This thesis will expand upon the work of Mr. Rhoby by comparing several additional fuel/air ratios at a much higher resolution to CFD results while also utilizing the next evolution of data fitting methods.

Research Objectives

Determine relevant scalar values of near-laminar flames using an IFTS for comparison to CFD and previous results. These additional data points are required to further validate and refine data reduction methods, provide a better understanding of laminar flame burners, and further validate IFTS as an efficient method to passively obtain spectral data and resulting scalar measurements.

Overview

This document will cover some background information of traditional methods for remote sensing spectroscopy, Fourier-Transform Spectroscopy (FTS), specific instruments used in the experiment, and relevant past work using the instrument. In addition the theory behind the single-layer radiance model used for this experiment will be covered along with a brief description of the CFD code utilized for comparison purposes. Methodology for the experiment will be covered in detail to include limitations faced. This will be followed by results and analysis showing where the model works well and where it breaks down and a conclusion.

II. Background and Theory

Background

Traditional Methods

Several methods of non-intrusive combustion diagnostics have been used in the past to identify temperatures, pressures, species concentrations, flow rates, etc. Some examples of laser based spectroscopy techniques include laser-induced polarization spectroscopy [5], planar laser induced fluorescence, and coherent anti-Stokes Raman scattering [4]. Basically, a laser is tuned to a specific frequency range enveloping natural resonance frequencies of a species of interest. In the case of laser-induced fluorescence, a laser operating in a tuned frequency range locally excites a point of interest which causes light to be emitted at specific frequencies from species with natural resonances in the frequency range. The frequencies and corresponding intensities of the emitted light can be used to determine temperature, species concentrations, etc. Raman

scattering uses inelastic scattering of photons to the same ends. Monochromatic light from a laser source is focused onto a gas. The polarizability of the subject atoms and molecules cause photon inelastic scattering, altering the photon frequency. These altered frequencies correspond to specific energy transitions of specific atoms/molecules in a particular state. The intensities of the transitions correspond to temperature, species concentrations, etc. of the subject gas. NASA's Glenn Research Center developed a method to provide quantitative measurements of major species concentration and temperature in high-pressure flames using spontaneous Raman scattering. Their goal is to provide a spontaneous Raman scattering calibration database. The lab apparatus required for this effort is quite extensive [6].

Fourier-Transform Spectroscopy (FTS)

Energy interacts with materials in a variety of ways. CO_2, for example, can occupy a multitude of atomic, vibrational, and rotational "states" depending on how much energy it has gained. When CO_2 transitions from a higher state to a lower one it will emit a photon with a frequency specific to that particular transition. All of the CO_2 transitions together form a "spectrum" of intensity vs. wavelength. All species present in a scene have their own spectrum which can yield temperature and concentration information.

An interferometer is a device (such as the Michelson interferometer shown in figure 1) that splits a light source beam, varies the optical path of the split beam, and then recombines the two beams to create interference patterns. This allows one to determine the frequency of light entering the device. Mapping the intensity of the light exiting the interferometer to wavelength creates an interferogram. This interferogram is the Fourier-

transform of the spectra of a scene. Thus, FTS involves taking the Fourier-transform of interferograms in order to produce a spectrum of a scene. Analyzing the spectrum allows determination of types of materials present (vegetation, water, man-made, etc) as well as species of gases and their temperatures and concentrations.

Telops Specifics

The Telops Hyper-Cam interferometer features a high-speed 320x256 indium antimonide (InSb) (1.5-5.5μm, 1200 Hz full-frame) focal-plane array (FPA) coupled with a Michelson interferometer [3]. Figure 1 shows a basic diagram of a Michelson interferometer.

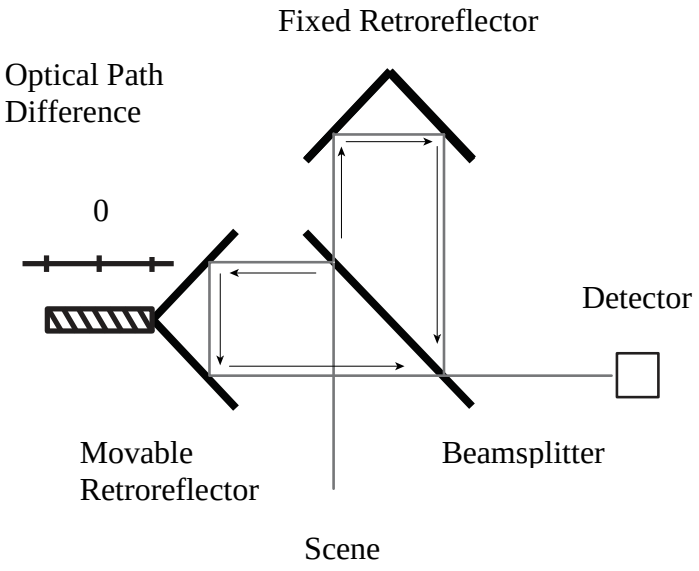

Figure 1: Michelson Interferometer Diagram

InSb is a type of semiconductor commonly used in thermal cameras, detecting light at a region of the spectrum dominated by thermal emission. Semiconductors are necessary components for any detector as they absorb the energy of incoming electromagnetic waves, converting them into carrier electrons. Each type of semiconductor is able to operate within a specific range of frequencies dependent upon

its particular atomic structure. The FPA of the Telops IFTS contains 81,920 individual InSb detectors arranged in a 320x256 grid, one for each pixel of the scene image.

Acquisition rate is a function of several parameters including spectral resolution, spatial resolution, instrument mirror speed, and integration time [3]. Spectral information is encoded as an interference pattern at each mirror position. The measured intensity is a resulting interference of all wavelengths. Spectral information for each of the mirror positions is collected to form spectral data "cube." This spectral cube contains a full spectrum (within InSb detection limits) for each pixel in the scene.

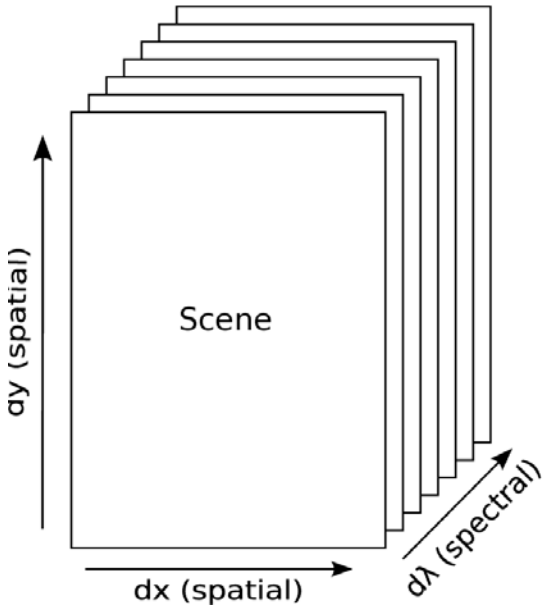

Figure 2: Interferogram cube representation where x and y axes are spatial (pixels) and λ is wavelength corresponding to optical path difference of the IFTS.

Hencken Burner Specifics

The Hencken burner used in this experiment is a non-premixed near-laminar flame burner often used for temperature calibration of other instruments. The cylindrical burner is composed of glass marbles and particulates in the lower region mixing each gas

in separate compartments in order to produce a consistent flow across the exit area of the burner. Air travels up through a 1 square inch (25.4 mm) of honeycomb structure providing approximately 480 oxidizer channels as seen in figure 3 below. About 173 stainless steel fuel tubes with 0.508 mm and 0.813 mm inside and outside diameters respectively are surrounded by six oxidizer channels resulting in fuel and air mixing just above the surface of the burner [7]. This mixture method helps reduce heat transfer into the burner as the flame does not touch the surface of the burner. The square flame region is bordered by a ¼ inch (6.4 mm) wide region of identical honeycomb structure used for inert gas co-flow, which helps stabilize the flow field and minimize entrainment of outside air [7].

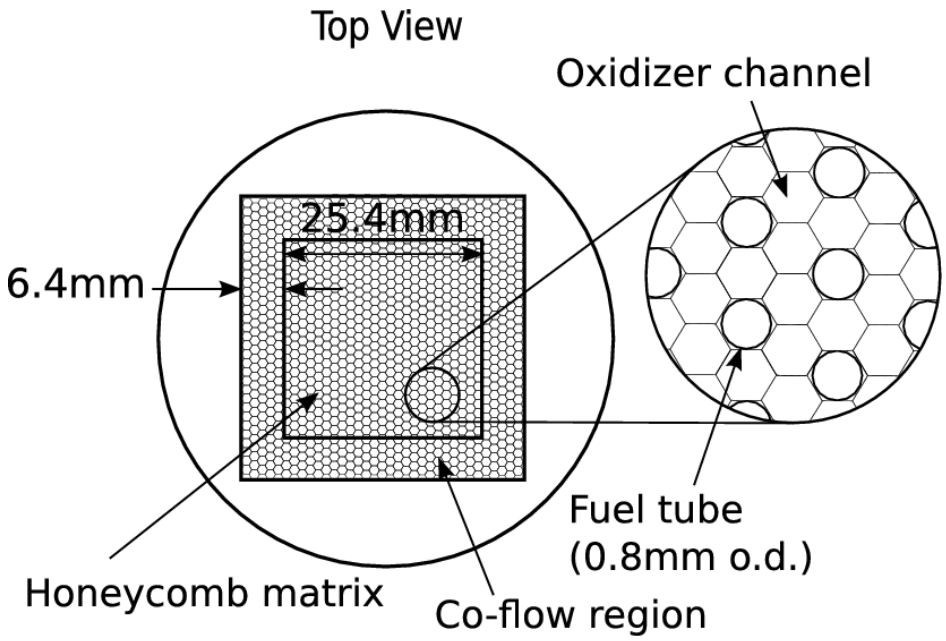

Figure 3: Hencken burner top view. ~173 fuel tubes with 0.813 mm outer diameter and 0.508 mm inner diameter, ~480 oxidizer channels

Remote Identification and Quantification of Industrial Smokestack Effluents via IFTS

Gross et al. demonstrated the usefulness of using IFTS to quantitatively measure the flow rates and species concentrations of smokestack emissions remotely. If developed further a lone operator could complete emissions compliance testing within a few hours with a complete set of calibrated plume measurements at his/her disposal. Temperature and species concentrations were estimated for the two-dimensional area just above the smoke stack with the use of a radiative transfer model. High resolution spectra enabled identification of CO_2, H_2O, SO_2, NO, HCl, and CO. Effluent concentrations were also accurately quantified. Additionally, spectral imagery retrieved from the IFTS system was shown to have promise in the study of fluid dynamics and atmospheric effluent dispersion.

Application of IFTS to Determine 2D Scalar Values in Laminar Flames

Rhoby et al. explored the usefulness of using an IFTS to analyze a laminar flame. The Telops IFTS was used to record two-dimensional spectral intensity measurements of an ethylene flame produced by a Hencken burner. Temperature and species concentrations were estimated at varying heights above the burner using a single-layer spectral model fit to IFTS data. Results correlated favorably with acCEAted intrusive and laser based measurement techniques [8]. Mr. Rhoby was also able to observe intensity fluctuations from vortices caused by buoyancy effects in the flame using the high speed infrared camera capabilities of the Telops IFTS. These results validated the use of the IFTS as a practical means for combustion diagnostics as well as highlighting its possible usefulness in flow field fluid dynamics.

CFD Modeling of flames

CFD modeling of laminar and turbulent flames has been explored extensively with the UNsteady Ignition and COmbustion with ReactioNs (UNICORN) Navier-Stokes based simulation program. UNICORN began in 1992 and has matured to the point where it can effectively model the diffusion characteristics of a pre-mixed flame. It has been used extensively in conjunction with many experimental tests and validated with laser diagnostics [9]. UNICORN provides the ability to model a large variety of jet flames from ignition to extinction and every time-step in between. Understanding combustion phenomena on a much deeper level than time-averaged results of the past is invaluable in the study of jet flames. UNICORN allows insight into combustion chemistry and buoyancy effects that were impossible to perceive with time-averaged single-point measurements [9].

Theory

Single-layer Spectral Model

The spectral radiance, $L(\tilde{\nu})$ from a non-scattered source in local thermodynamic equilibrium can be approximated by

$$L\left(\tilde{\nu}\right) = L_{bg}\left(\tilde{\nu}\right)e^{-\int_0^s k(\tilde{\nu},s')ds'} + \int_0^s k(\tilde{\nu},s')B\left(\tilde{\nu},T(s')\right)e^{-\int_{s'}^s k(\tilde{\nu},s'')ds''}ds', \qquad (1)$$

where $L_{bg}\left(\tilde{\nu}\right)$ is the background spectral radiance and $k(\tilde{\nu},s')$ is the absorption coefficient. The first term gives the radiance of the background modified by attenuation through the source. Strong absorbers are also strong emitters. Thus, in the optically thin

limit, $k(\tilde{\nu},s')ds'$ is the gas emissivity at s' and $B(\tilde{\nu},T)$ is Planck's blackbody radiance at temperature (T), $B_{\tilde{\nu}}(T)=2hc^2\tilde{\nu}^3\frac{1}{\exp[hc\tilde{\nu}/(k_BT)]-1}$. In the second term, $k(\tilde{\nu},s')B\left(\tilde{\nu},T(s')\right)ds'$ represents the photons born at the point s'. The exponential, $e^{-\int_{s'}^{s}k(\tilde{\nu},s'')ds''}$ accounts for the attenuation of these photons through the remainder of the source (i.e. Beer's law). If the source can be approximated as a single homogeneous layer, (1) can be approximated as

$$L\left(\tilde{\nu}\right)=\tau\left(\tilde{\nu}\right)\varepsilon\left(\tilde{\nu},\xi_k\right)B\left(\tilde{\nu},T\right), \tag{2}$$

where $\tau(\tilde{\nu})$ is the atmospheric transmittance between the flame and the instrument. Atmospheric transmittance is the frequency dependent coefficient of light that is not absorbed by the atmosphere for a given path length and atmospheric conditions and can be approximated using the high-resolution transmission (HITRAN) molecular absorption database. $\varepsilon(\tilde{\nu},\xi_k)$ is gas emissivity, a function of wave number, $\tilde{\nu}$ and gas mole fraction, ξ_k.

Background radiation is negligible and is ignored in this simplified model. Temperature and gas concentrations are found from the expression for emissivity,

$$\varepsilon(\tilde{\nu})=1-\exp[-(\sum_k\xi_k\sigma_k(\tilde{\nu},T))Nl], \tag{3}$$

where $N=P/\left(k_BT\right)$ is the gas number density, l is the optical path length through the flame, and σ_k is the Boltzmann-weighted absorption cross-section for a particular species *k* at temperature T. Line-by-Line Radiative Transfer Model (LBLRTM) [12] along with the high-temperature extension of the HITRAN spectral database [13,14] are used to compute CO_2 and H_2O absorption cross-sections.

Equation (2) was used to fit the LBLRTM generated spectrum to collected data in the 3100 to 3500 cm^{-1} spectral region. This region contains emission lines from both CO_2 and H_2O while also having minimal atmospheric signal attenuation due to absorption. The chosen spectral envelope also benefits from being optically thin, which allows light from the interior of the flame to travel out to the instrument. There is also no instrument self-emission, meaning the subject spectral region isn't changed by thermal emission from the instrument itself.

From (3) and (2) it can be seen as species concentrations ξ_k increase so does emissivity $\varepsilon(\tilde{\nu}, \xi_k)$ which in turn increases spectral radiance $L(\tilde{\nu})$. Spectral radiance will also increase with temperature due to the blackbody radiance temperature dependence.

2-D CFD Model

UNICORN utilizes an axis-symmetric, time-dependent mathematical model that solves conservation equations for momentum, enthalpy, continuity, and species [9]. The model performs these calculations at user specified grid points and a constant time-step. The results for each grid point at each time-step are calculated from adjacent grid points and previous time steps, eventually iterating to reach an accurate representation of a real flame. The governing equations and a more detailed description of how UNICORN functions have been described by Roquemore [9] and Katta [15,16,17] et al.

III. Methodology

IFTS Setup

The general lab setup is illustrated in Figure 2Figure 4(a) below.

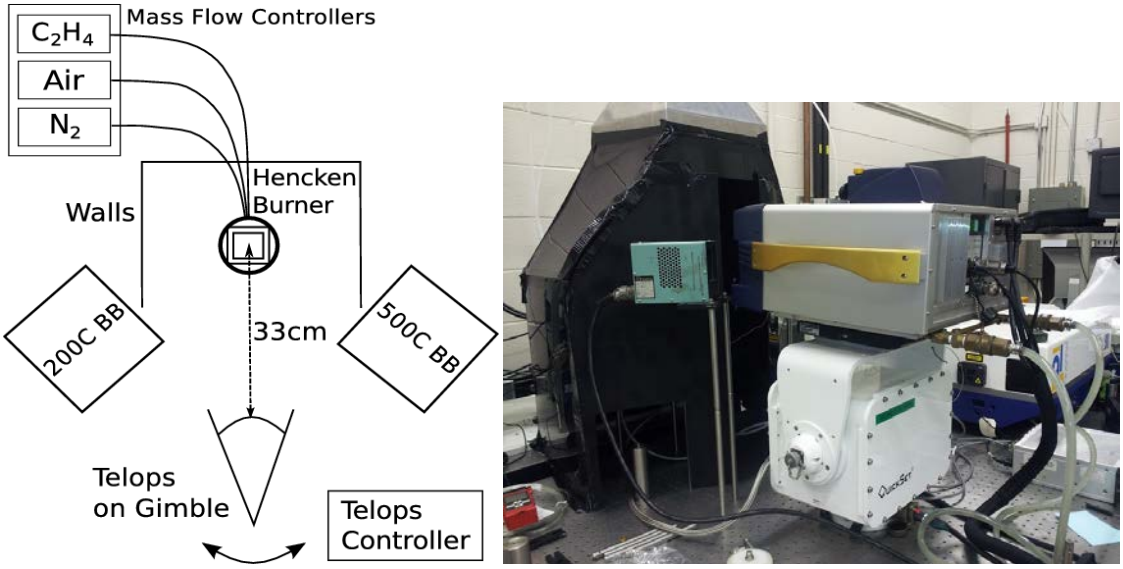

Figure 4: (a) Experimental Setup (not to scale). (b) Picture of setup

The Hencken burner was placed level with the line of sight of the Telops IFTS and surrounded by cardboard walls painted flat black to minimize both outside air current interaction and reflections or other light sources, Figure 4(b). The walls were tapered above the flame up to a vent which removed exhaust gases.

Two blackbodies were placed on either side of the walled off burner area to provide calibration sources. The blackbody on the left, an Electro Optical Industries CES200, was set at 200°C. The other, a LES600 series blackbody, was set at 500°C. The CES200 has emissivity of 0.97 ±0.02 while the LES600 has emissivity of 0.94 ±0.02. These blackbodies were placed on either side of the walled off burner area. Due to an excessive amount of heat produced from the 500C blackbody and its close

proximity to the Telops instrument, a flat black metal plate was used as a heat shield when data was not being collected from the blackbody.

MKS Instruments ALTA digital mass flow controllers (model no. 1480A01324CS1BM) connected to a MKS Instruments Type 247 4 Channel Readout control unit were used to regulate the flow of the ethylene, air, and nitrogen co-flow in standard liters per minute (SLPM) per Table 1. SLPM is a flow rate corrected to standard atmospheric pressure and temperature. After allowing the mass flow control unit to reach equilibrium operating temperature the mass flows were adjusted using a Bios International Definer 220-H (Rev C) flow meter to fine tune mass flow. Mass flow settings were duplicated from the work of Meyer et al. [8] in order to provide an accurate comparison to the authors' diode-laser-based UV absorption sensor spectroscopy results.

Table 1: Gas Flow, Standard Liters per Minute (SLPM) and Corresponding Fuel-Air Equivalence Ratio (Φ)

Φ	C_2H_4 SLPM	Air SLPM	N_2 Coflow SLPM
0.81	0.69 ±0.005	12.2 ±0.05	12.0 ±0.05
0.91	0.78 ±0.005	12.2 ±0.05	12.0 ±0.05
1.11	0.95 ±0.005	12.2 ±0.05	12.0 ±0.05

Fuel-air equivalence ratios were derived from

$$\phi = \frac{\text{fuel to oxidizer ratio}}{(\text{fuel to oxidizer ratio})_{\text{stoichiometric}}} = \frac{(n_{\text{fuel}}/n_{\text{ox}})}{(n_{\text{fuel}}/n_{\text{ox}})_{\text{stoichiometric}}} \ , \tag{4}$$

where n is number of moles. For a stoichiometric ethylene-air reaction, $C_2H_4 + 3(O_2 + 3.76N_2) \rightarrow 2CO_2 + 2H_2O + 3.76*3N_2)$, the fuel to oxidizer ratio of moles is

$$(\text{fuel to oxidizer ratio})_{\text{stoichiometric}} = \frac{1}{3(1+3.76)} = 0.07 \ , \tag{5}$$

If we want Φ to be 0.91 then from (4) and (5), the fuel to oxidizer ratio would have to equal 0.064. Setting air flow equal to 12.2 SLPM we simply multiply by 0.064 to arrive at the fuel SLPM of 0.78.

The Telops IFTS was placed on top of a Moog QuickSet pan and tilt system to ensure a consistent scene after rotating to collect interferogram data cubes from both blackbodies. The Telops was fitted with near-field optics allowing the instrument to focus on a scene as close as 31cm away. The Telops was then set up with 33 cm from the center of the Hencken burner flame to the front lens of the optic. Due to the intensity of the flame and blackbodies a Spectrogon ND-IR-1.45 (25.4x1 mm) neutral density germanium filter was used to keep the FPA from reaching saturation. The Telops was set to a 128x200 pixel (~61x95mm) spatial resolution with 55 ms integration time and 0.5 cm^{-1} spectral resolution. 32 interferogram cubes were collected for each blackbody and flame. Each set of 32 cubes was then averaged together to produce an average interferogram for each of the 25,600 pixels.

IFTS Setup Limitations

Due to physical space limitations of the laboratory the flame enclosure was not perfectly symmetric with small cut-outs for immovable equipment from past experiments. The hood vent fan was set to its lowest setting to minimize its effects on the flame flow field. However, the resulting exhaust mass flow for this setting was not measured. As a result, asymmetric airflow at an unknown but assumed small velocity into the enclosure from the outside region could have affected the flames' flow fields.

Calibration Method

The following method was developed by Dr. Gross et al [1,2,3,10]. The optical path difference (x) between two beams is varied using an interferometer, in this case, the built-in Michelson interferometer. The resulting image intensity $I_{i,j}$ varies based on the spectrum $L_{i,j}(\tilde{\nu})$ as

$$I_{i,j} = \frac{1}{2}\int_0^\infty \left[1+\cos\left(2\pi\tilde{\nu}x\right)\right] G\left(\tilde{\nu}\right) L_{i,j}\left(\tilde{\nu}\right) d\tilde{\nu} = I_{DC} + I_{AC}(x) \ , \tag{6}$$

where i and j refer to FPA location (or pixel coordinates) and $G\left(\tilde{\nu}\right)$ is the instrument response, to include the spectral quantum efficiency of InSb. Spectral quantum efficiency is the frequency dependent percentage of photons impacting the semiconductor which are converted to carrier electrons. I_{DC} represents the broadband spectrally-integrated signal while $I_{AC}(x)$ is the modulated component. The constant, I_{DC}, combined with $I_{AC}(x)$ make up an interferogram, $I_{i,j}(x)$, for a static scene.

The spectrum, $L_{i,j}(\tilde{\nu})$ is created from a standard calibration [11] of the Fourier-transformation of these $I_{i,j}(x)$ interferograms and is shown in Figure 5 below for the Φ = 0.91 flame at 5 mm above the burner surface. The finite maximum optical path difference, $OPD_{\max} = x_{\max} - x_{\min}$, has the effect of essentially multiplying the interferogram by a rectangle function of width, $OPD_{\max}$. This convolves the monochromatic spectrum with the instrument line shape function in the Fourier domain, $ILS(\tilde{\nu}) = 2(OPD_{\max})\,\mathrm{sinc}(2\pi\tilde{\nu}(OPD_{\max}))$, limiting spectral resolution but smoothing the spectrum thereby reducing "false" features caused by instrument noise.

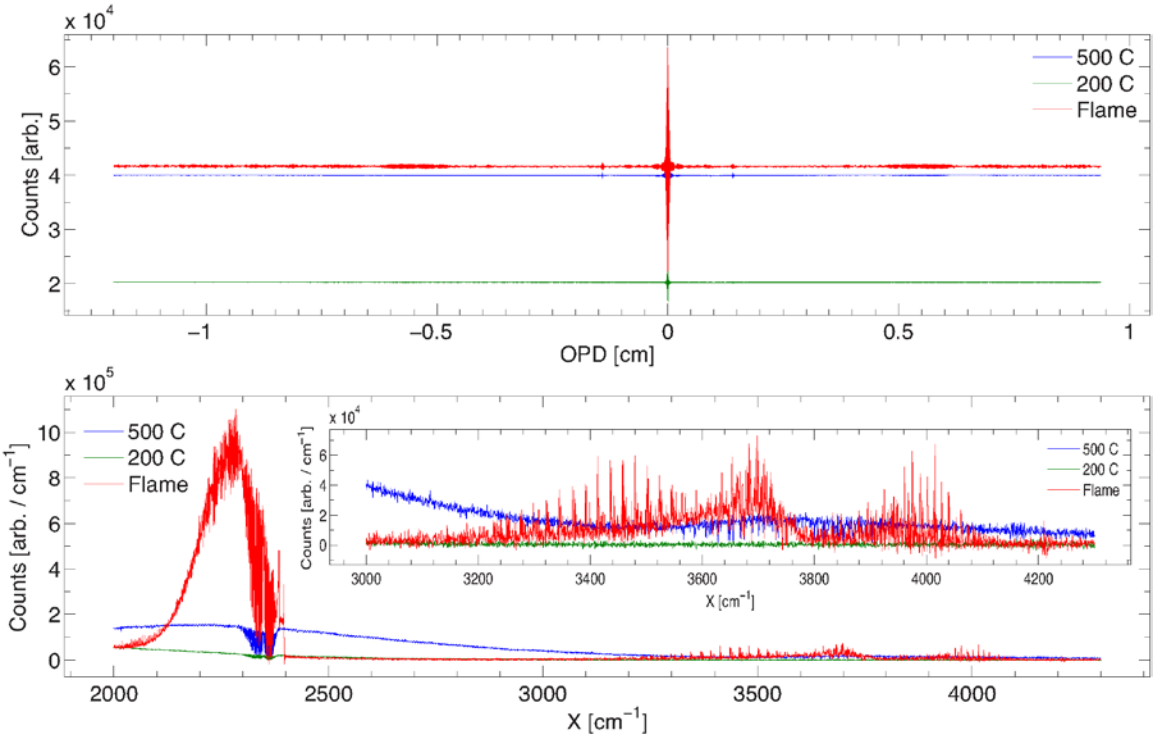

Figure 5: Top: interferograms of Φ =0.91 flame at 5mm above burner surface and two blackbodies. Bottom: Raw spectrum from Fourier-Transform of interferograms.

The figure above may seem abnormal to some as traditional temperature calibration normally uses high and low known temperature sources to sandwich the raw data. However, spectral calibration uses the entire spectrum for calibration. The area under the spectrum provides the overall intensity "seen" by the interferometer. The 500 °C blackbody provided a similar amount of intensity, nearly saturating the interferometer, as the 2000 °C flame. It may appear that our raw signal has a higher intensity due to the large feature in the 2000 to 2400 cm^{-1} region but the 500 °C blackbody curve makes up the area difference over the rest of the spectrum.

Nominally, a band pass filter would be used to remove CO_2 spectral features in the 2000 to 2400 cm^{-1} region. However, this filter was unavailable for use during the limited time the instrument was available to me. These additional CO_2 features

introduced a lot of signal to a part of the spectrum that was not used for fitting, thus introducing more noise into the system. If the filter were used the instrument's integration time setting could have been increased without saturating the FPA, resulting in greater signal to noise ratio for the spectral region of interest and therefore increasing fitting accuracy.

The CO_2 features in question could not be used in the fitting process due to atmospheric absorption causing calibration problems in that region. Atmospheric absorption bands caused portions of the raw spectrum's intensity to drop close to zero as seen in the top part of Figure 6 below. Calculating radiance involved dividing by these near zero intensities resulting in large false spikes in the spectrum in regions of high absorption and very low signal, seen in the bottom part of Figure 6.

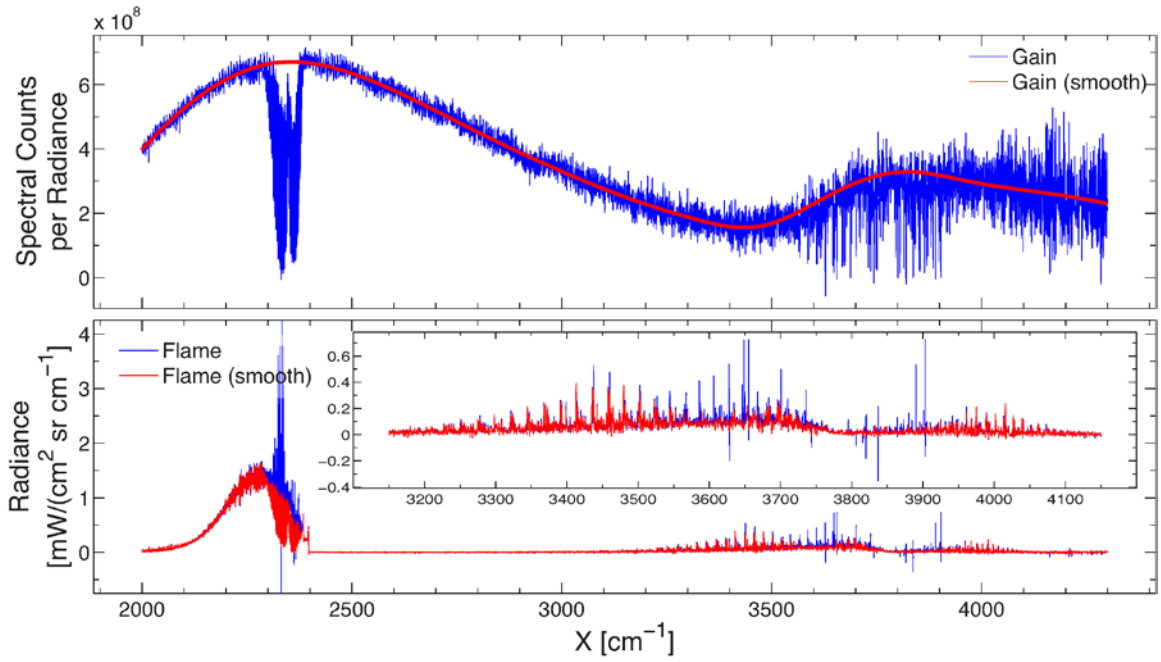

Figure 6: Top: Gain curves used for calibration in counts per radiance. Blue gain curve was used for this document's results. Red smooth gain curve was developed afterward. Bottom: Resulting radiance from calibrating with each gain curve. Blue spectrum was used for this document's results.

The smooth gain curve in the above figure was developed after the results presented in this document revealed these calibration problems. The spectral window used for fitting had to be limited from 3100 to 3500 cm^{-1} in order to cut out the majority of false spectrum spikes. Using a larger window would have allowed more accurate fitting results by giving the model more spectral features to work with.

CFD Setup

UNICORN utilizes ASCII text files as inputs to set up an experiment model. The Hencken burner setup was approximated by stipulating mass fractions of fuel, air, and water vapor, as well as their temperatures and velocities. Geometry of air-fuel, co-flow region, and atmospheric air were input as "cards" with each card length determined from the center of the flame. For example, the air/fuel mixture card length was set at 1.27 cm (1/2 inch) and co-flow card length at 1.89 cm (or 0.64 cm from the end of the air/fuel region at 1.27 cm). Two grid systems were utilized: one assuming there were no walls and one including a wall boundary 33 cm away from the flame.

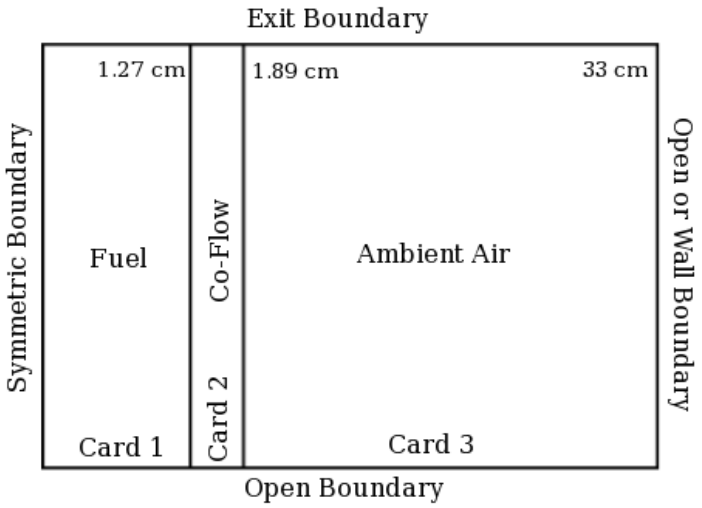

Figure 7: Schematic of UNICORN CFD card setup.

Due to space limitations, 33 cm was about as far as the hood walls could be moved away from the burner. The farther away the walls can be placed the less affect they will have on airflow around the flame. In the area of interest near the base of the flame the difference between the two results was negligible. The grid system with no walls was used for the remainder of the simulations since each run completed 3 times faster than the grid system with walls.

An initial run without swirl or buoyancy effects is normally required to allow UNICORN to perform calculations and determine initial flame properties without diverging. In this case a first run of 1000, 0.5 ms time step iterations was effective in providing a starting point for a second run with more complex flame dynamics turned on. This second run consisted of 20,000, 0.5 ms time step iterations. At 15,000 iterations the flame is well established and in a "stable" condition. Average flame data were calculated from the last 5,000 time steps (15,000 to 20,000).

CFD Setup Limitations

The multitude of fuel tubes and honeycomb oxidizer channels in three-dimensional space was too complex to setup in the two-dimensional UNICORN code. Therefore, the air-fuel and co-flow regions were modeled as concentric tubes with the air-fuel being premixed. Also, since UNICORN is a 2-D simulation the flame is assumed to be axis-symmetric with the burner base being circular. The Hencken burner however is square at the base contributing to some differences between IFTS and CFD data, especially at the edge of the flame near the burner surface. The velocity of the ambient air around the outside of the burner was unknown and approximated as 0.01 m/s upwards.

IV. Analysis and Results

Data Overview

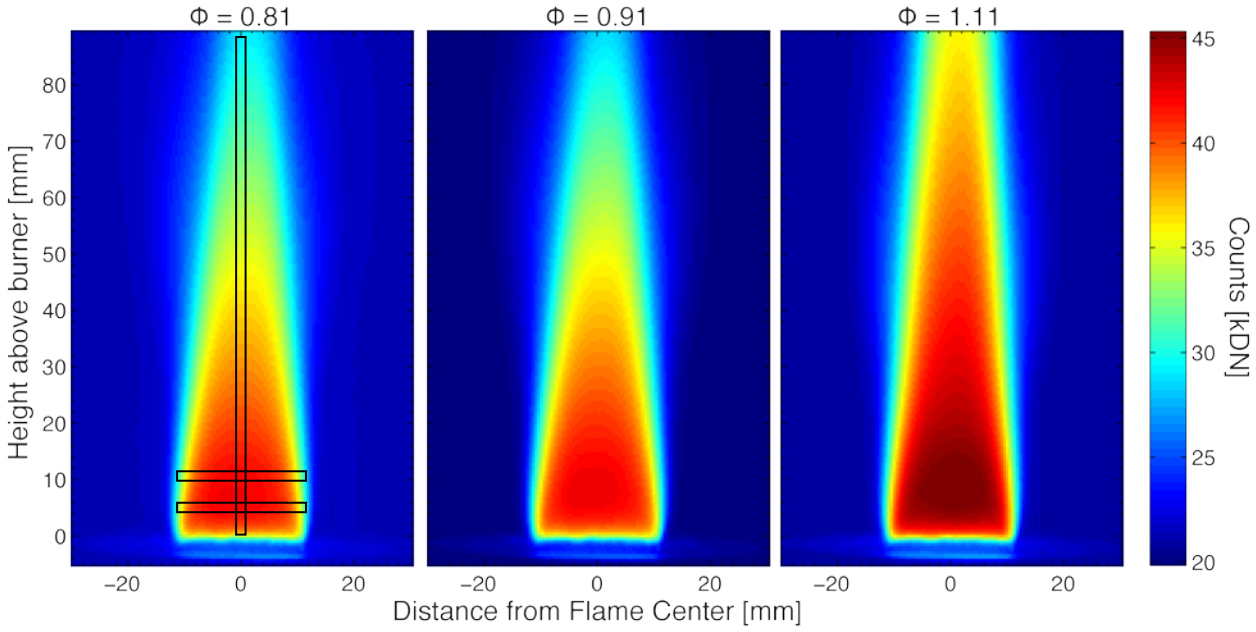

Figure 8: Averaged flame intensities created from averaging 32 IFTS interferogram data cubes. Rectangles represent the lines of pixels that were fit to the model vertically and at 5 and 10 mm above the burner surface for each flame.

The above figure shows the IFTS observed average flame intensities (arbitrary units) for each of the three fuel-air equivalence ratio (Φ) flames observed. The flame is said to be stoichiometric if the fuel-air equivalence ratio is equal to one. This means there is just enough air to allow all of the fuel to burn. Φ values less than one describe a flame that has too much air (fuel lean) resulting in un-reacted oxidizer which has the effect of cooling the overall flame temperature and thus lowering the average intensity observed by the IFTS. Φ values greater than one describe a flame that doesn't have enough air or is fuel rich. Un-burnt fuel exists in the flame because it has no oxidizer to react with. As the flame travels upward buoyancy effects cause the flame to accelerate

upward. The center of the flame has higher temperatures than the outside edges of the flame causing the interior of the flame to accelerate faster than the exterior. Vortices are formed from this velocity differential, as shown in Figure 9, and their circular motion brings in outside air. This outside air then reacts with the un-burnt fuel causing the flame to be much taller and have a higher temperature, increasing the average intensity. Flame widths are approximately the same due to geometry of the burner, vertical mass flow direction, and buoyancy effects causing mostly vertical gas acceleration and expansion.

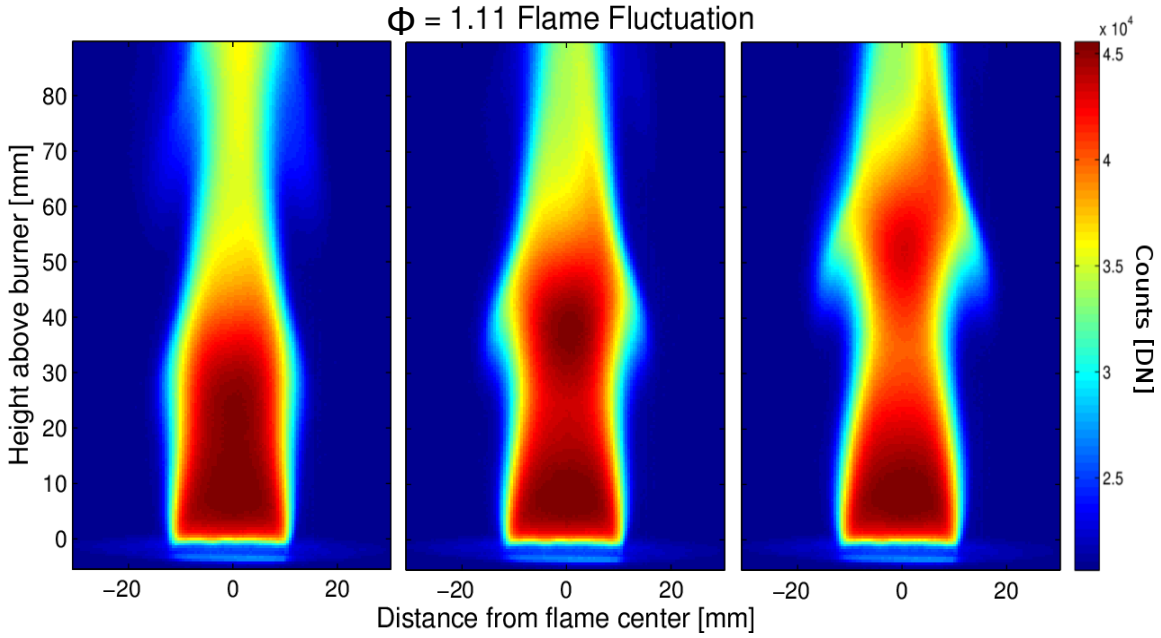

Figure 9: Example of flame fluctuation of Φ = 1.11 flame, taken from 3 single frames of an IFTS interferogram data cube. Buoyancy effects cause vortices, seen developing from left-most frame to right frame, which entrain outside air causing further reactions with un-burnt fuel, raising flame height and temperature.

Figure 9 shows three snapshots of the Φ = 1.11 flame produced from a single interferogram data cube. Each image is raw intensity data recorded by the IFTS at a specific Michelson mirror position. Further analysis of this high speed imagery could be

utilized for flow field dynamics information such as intensity fluctuation rates due to buoyancy.

The figure below shows the raw average spectrum for the three flames obtained using the Telops IFTS.

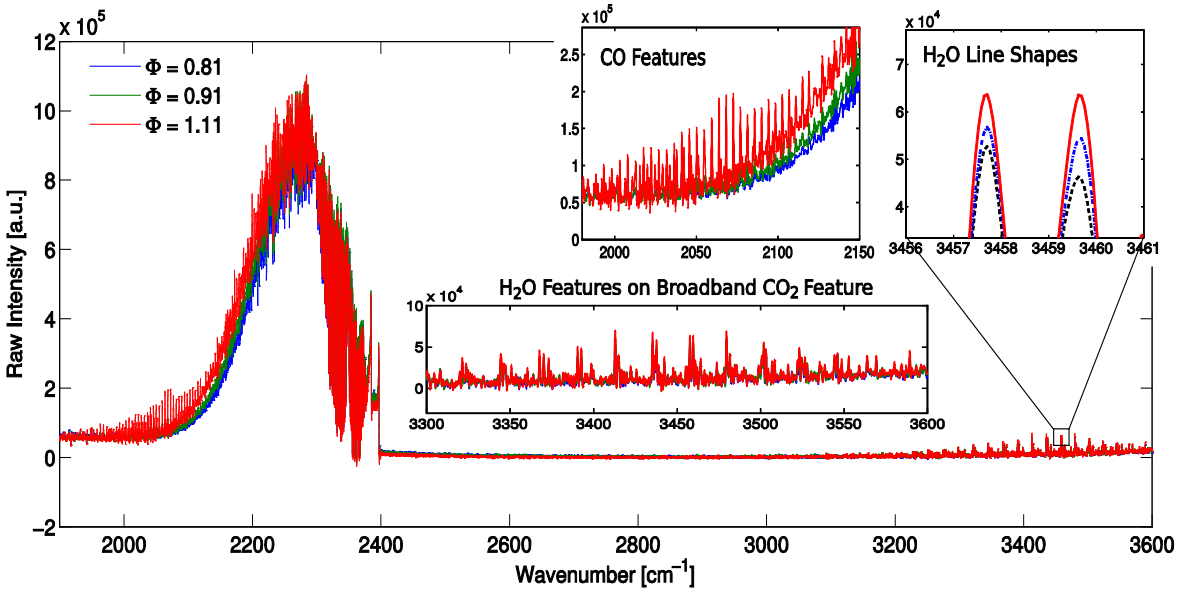

Figure 10: Full spectrum for all three flames at flame center, 5 mm above burner surface. Spectral features rise in height as flame intensity increases. This is due to increases in temperature and species concentrations.

The large feature on the left side is the 4.3 µm asymmetric stretch feature of CO_2. The downward slope from ~2300 to 2400 cm^{-1} is a result of atmospheric CO_2 absorption. Some features such as CO spectral lines around 2075 cm^{-1} are much taller for the $\Phi = 1.11$ flame. This is due to the higher Φ flame being fuel rich, leaving more un-reacted CO in the region of the flame near the burner surface. These CO features all but disappear as we travel upwards in the flame where entrainment of outside air causes further chemical reactions. Taller line shapes resulting from both increased temperature

and species concentration are also seen in the H_2O symmetric and asymmetric stretching mode features on the right side of the figure from about 3250 cm^{-1} to 3600 cm^{-1}.

Qualitatively the general features of each spectrum appear similar. However, there are distinct differences such as relative line heights of water emission features shown in the rightmost expanded part of Figure 10. One can see an obvious pattern in line shape height for the three flames with regard to fuel-air equivalence ratio, Φ. To explore the nature of these changes further, spectrums were generated in the H_2O structured emission region using the model at ideal temperature and H_2O concentration as well as ±20% change to temperature and ±20% change to H_2O concentration. The spectral contribution from CO_2 is minimal as seen in part (a) of the figure below and is thus not considered further. Part (b) of Figure 11 shows how temperature and H_2O concentration changes affect the spectrum separately.

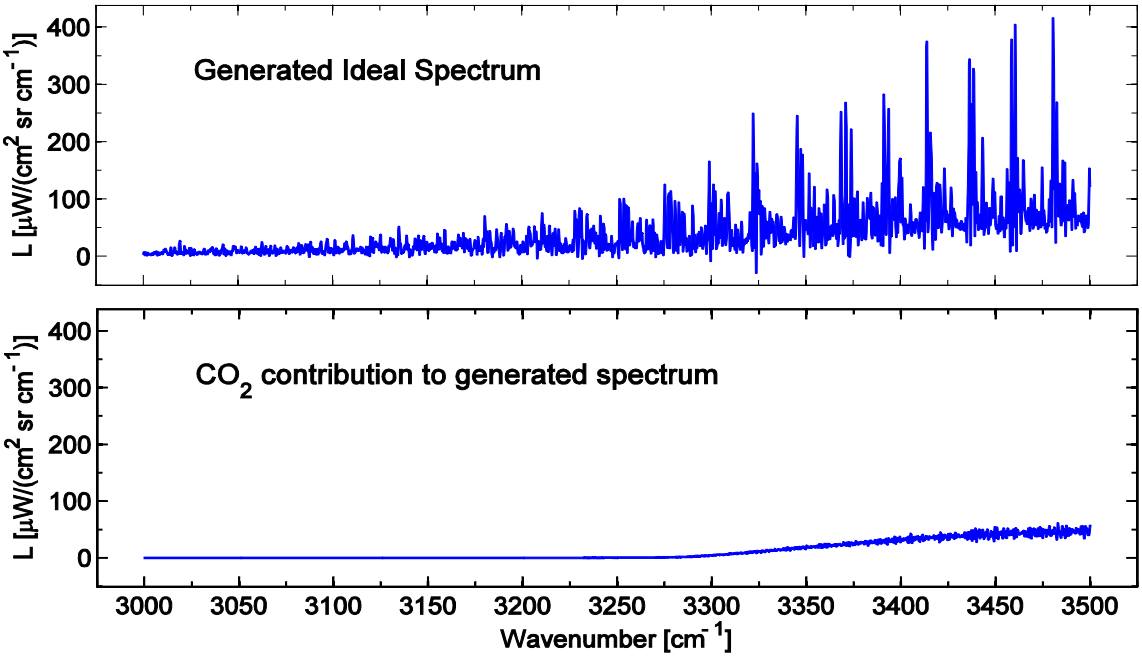

(a)

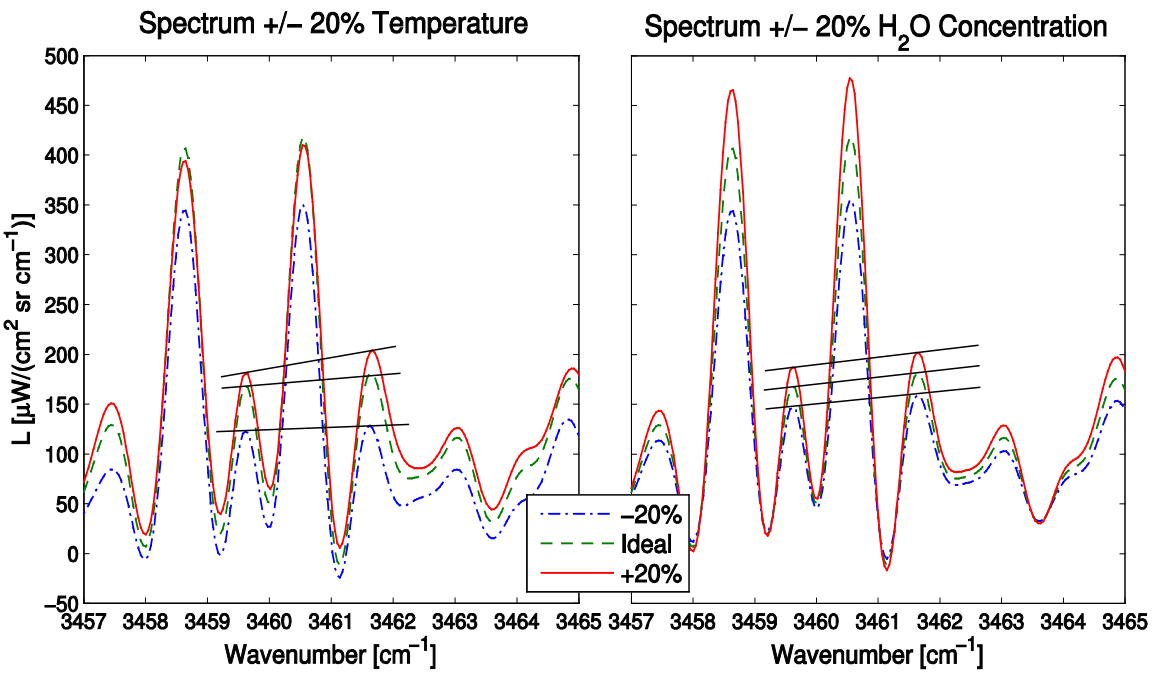

(b)

Figure 11: (a) Generated spectrum and CO_2 contribution for ideal Φ = 0.91 flame at equilibrium. (b) Comparison of model generated spectrum for ideal flame to generated spectrums at ±20% temperature and H_2O concentration. Temperature increase does not raise line shapes linearly because its relation to the model is exponential. H_2O concentration increase raises line shapes linearly.

As expected, increasing temperature increases line shape height. However, this increase is not the same from feature to feature resulting in increasing slopes of lines drawn between the peaks. This is due to temperature being related to the model exponentially and being frequency dependent. Changes to H_2O concentration on the other hand result in similar changes between line heights, illustrated by nearly parallel lines drawn from peak to peak. Taking a Taylor series expansion of Equation 3 in the optically thin limit gives $\varepsilon(\tilde{\nu}) = Nl\sum_k \xi_k \sigma_k(\tilde{\nu},T)$, showing concentration, ξ_k, has a linear relationship to emissivity and spectral radiance. Also of note is temperature changes shift the entire spectral line while concentration changes only seem to change the peak heights.

IFTS Fitting the Model

Temperature and species concentrations were varied within the single-layer model outlined in the theory section (2.2.1) in order to fit an LBLRTM generated spectrum to the spectrum data collected by the IFTS. The figure below shows a single pixel example of this data fit and corresponding fit residuals from Φ = 0.81 flame at flame center 5 mm above the burner surface. Fit residuals are the difference between the model fit and spectral data. Fit residuals showing no structure through the frequency range indicate low systematic error in the result. Units for the calibrated spectrum, $L(\tilde{\nu})$ in this case is spectral radiance [μW/(cm^2 sr cm^{-1})].

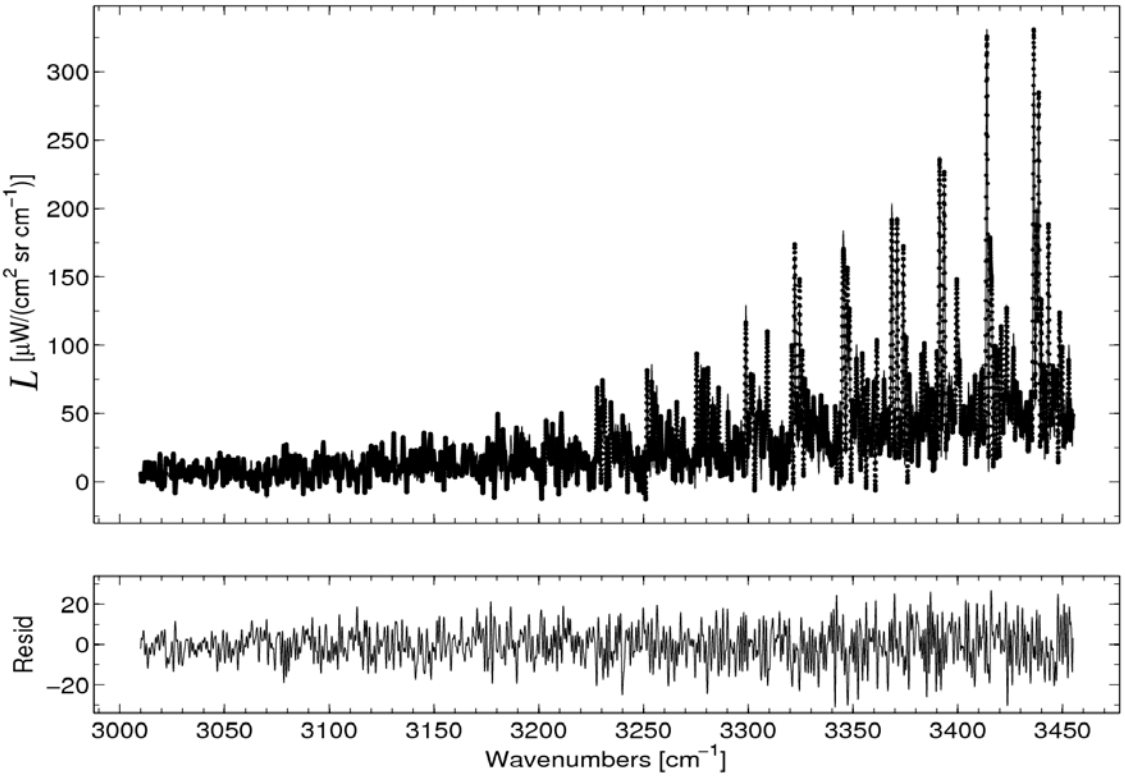

Figure 12: Example of spectral data fit (top) with residuals (below). Dots represent IFTS data. Lines are from the LBLRTM generated model. This example is the center pixel fit at 5 mm above burner surface for Φ = 0.81 flame. Unstructured residuals indicate low systematic error in the fit.

The figure above is a typical fitting result for the two rows of pixels fit horizontally at 5 and 10 mm above the burner surface as well as vertically up to about 20 mm above the burner surface for all three flames. All of the figures in this region looked very similar to Figure 12 with little to no structure of the residuals. Model fits in regions of lower intensity resulted in noticeable differences between data and model with larger residuals. The figure below shows the root mean squared error of each pixel's spectral model fit for a horizontal profile of the Φ = 0.91 flame at 10 mm above the burner surface.

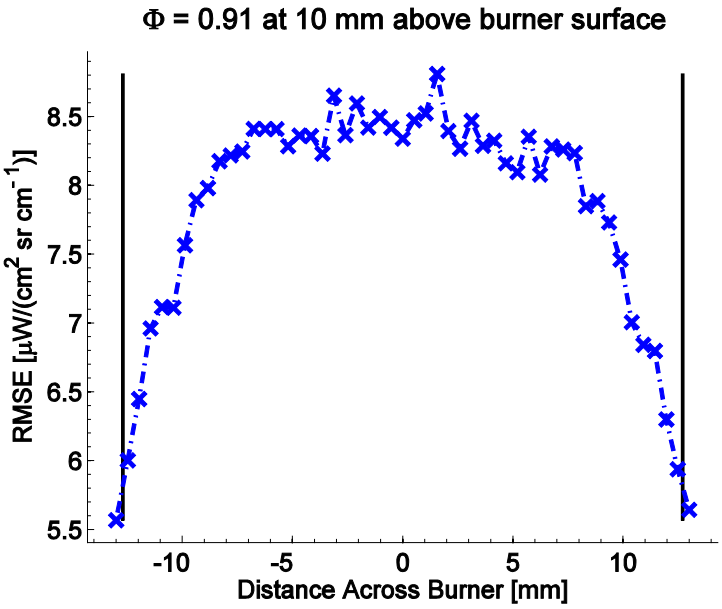

Figure 13: RMSE of each pixel's spectral model fit for Φ = 0.91 flame at 10mm above burner surface. Vertical lines denote location of edge of burner.

RMSE includes instrument noise as well as spectral model fit error. As the flame's spectral radiance drops at the edge of the flame the error contribution from the data fit is also reduced.

Fitting Results

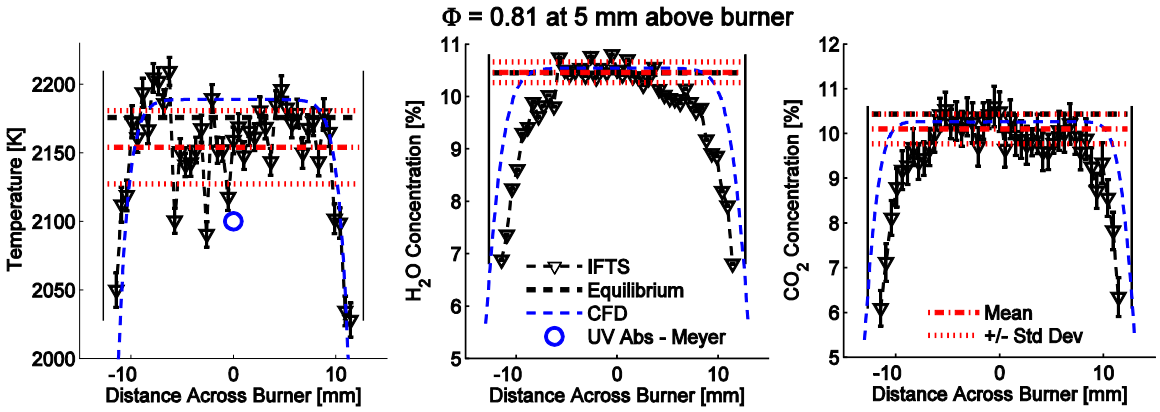

Figure 14: Temperature (left), H_2O concentration (center), and CO_2 concentration (right) for Φ = 0.81 flame at 5 mm above burner surface compared to NASA-Glenn Chemical Equilibrium Program produced values and previous diode-laser-based UV absorption results from Meyer et al. Vertical lines denote location of edge of burner. Blue dashed line is UNICORN CFD result.

Temperature fit results for the Φ = 0.81 flame at 5 mm above the burner surface, although somewhat inconsistent pixel to pixel, are relatively close to the ideal equilibrium value though slightly low in the center of the flame. H_2O concentration fit values on the other hand are slightly high in the middle of the flame. Equilibrium values were generated using NASA-Glenn Chemical Equilibrium Program (CEA) and are denoted in figures by horizontal dashed lines. UNICORN CFD results compare favorably to CEA equilibrium values and are represented by the blue dashed line. Vertical solid lines indicate the end of the fuel/air region of the Hencken burner. Mean and standard deviation lines were computed from pixels ±5 mm from center of burner.

Results for the Φ = 0.81 flame at 10 mm above the burner surface in the figure below show similar tendencies, though accentuated more with lower center flame temperatures and higher H_2O concentrations.

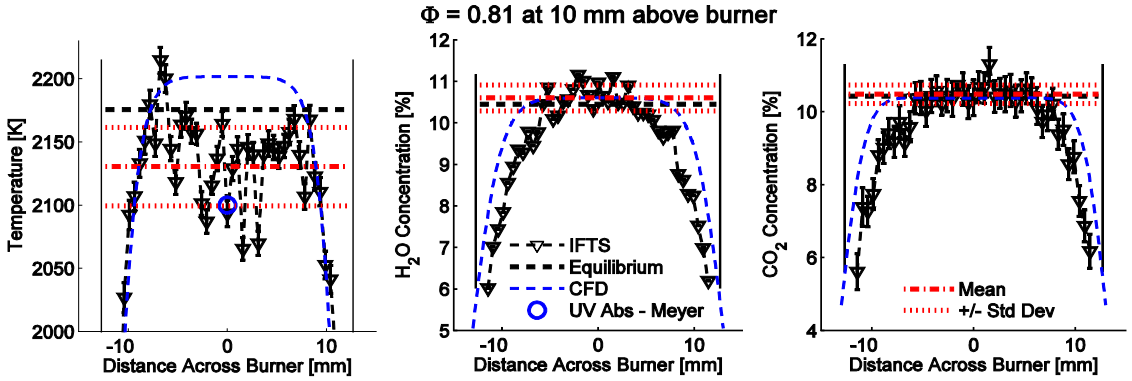

Figure 15: Temperature (left), H_2O concentration (center), and CO_2 concentration (right) for Φ = 0.81 flame at 10 mm above burner surface compared to NASA-Glenn Chemical Equilibrium Program produced values and previous diode-laser-based UV absorption results from Meyer et al. Vertical lines denote location of edge of burner. Blue dashed line is UNICORN CFD result.

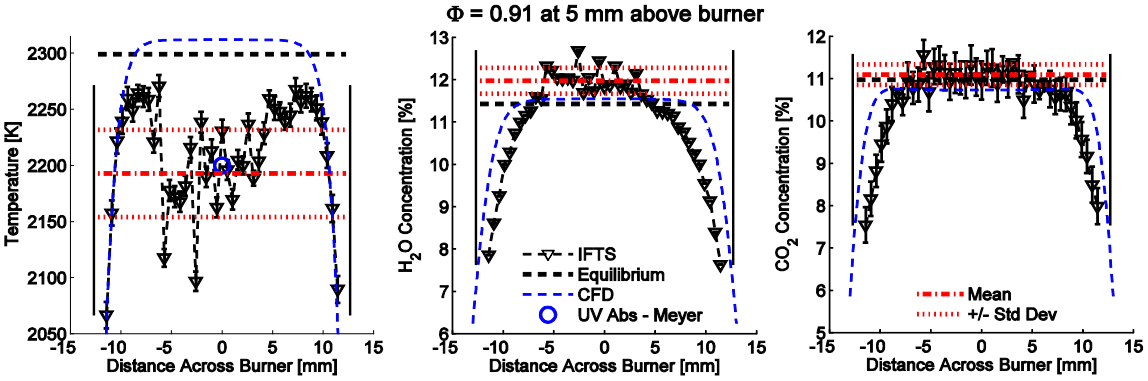

Figure 16: Temperature (left), H_2O concentration (center), and CO_2 concentration (right) for Φ = 0.91 flame at 5 mm above burner surface compared to NASA-Glenn Chemical Equilibrium Program produced values and previous diode-laser-based UV absorption results from Meyer et al. Vertical lines denote location of edge of burner. Blue dashed line is UNICORN CFD result.

Figure 16 continues to show a tendency for the fit to conclude with a lower temperature and high H_2O concentration in the center of the flame than the equilibrium value. CFD results match well with equilibrium values but indicate higher H_2O concentrations approaching the edge of the flame with a curve that rolls off later than IFTS fit values. Center temperature values match well with Meyer's diode-laser-based

UV absorption results, which have been consistently lower than NASA-Glenn CEA equilibrium values

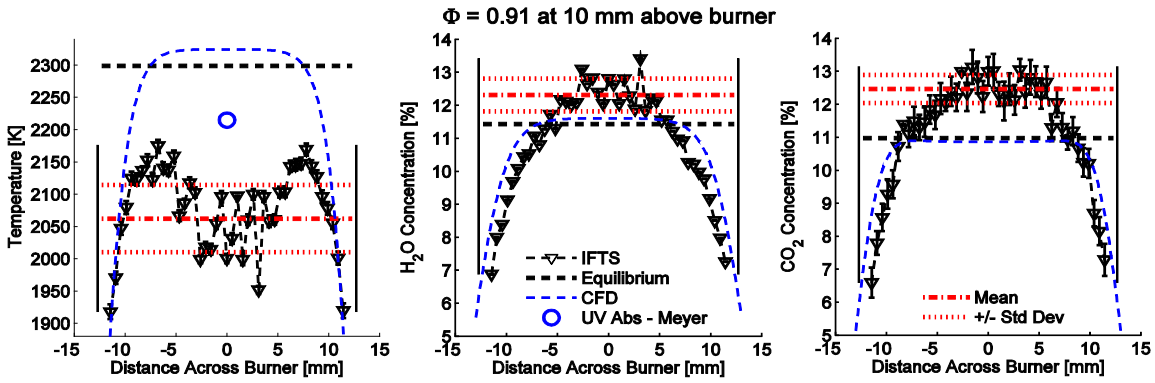

Figure 17: Temperature (left), H_2O concentration (center), and CO_2 concentration (right) for Φ = 0.91 flame at 10 mm above burner surface compared to NASA-Glenn Chemical Equilibrium Program produced values and previous diode-laser-based UV absorption results from Meyer et al. Vertical lines denote location of edge of burner. Blue dashed line is UNICORN CFD result.

Figure 17 reveals even lower temperature fit results for the Φ = 0.91 flame, while CO_2 fit concentrations are higher than CFD and equilibrium values. H_2O concentrations should be lower at 10 mm than at 5 mm above the burner surface. These results indicate H_2O concentrations slightly higher than the 5 mm case. Once again the concentration values begin to roll off sooner than CFD predicted results.

Results for Φ = 1.11 flame shown in Figure 18 reveal a continued trend of progressively lower temperature and higher H_2O and CO_2 concentration fit values in the center region of the flame. Excluding the obvious outlier pixel, there is an apparent correlation between low temperatures and high concentrations.

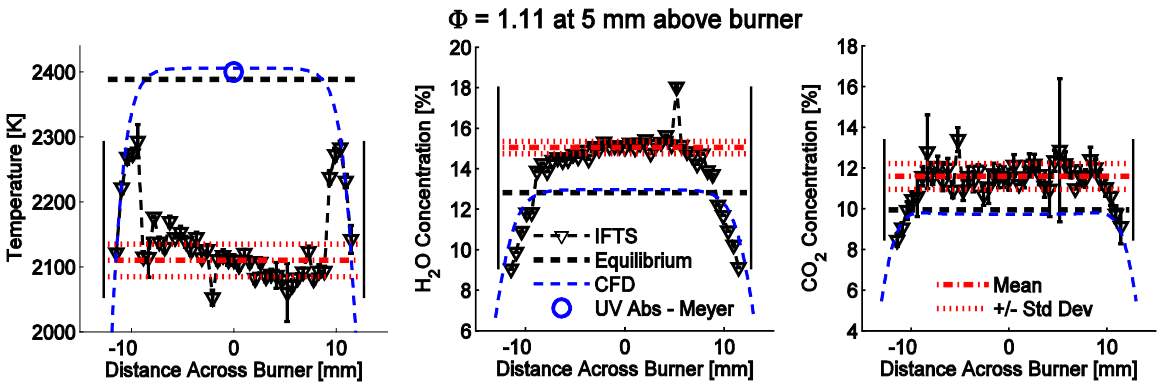

Figure 18: Temperature (left), H_2O concentration (center), and CO_2 concentration (right) for Φ = 1.11 flame at 5 mm above burner surface compared to NASA-Glenn Chemical Equilibrium Program produced values and previous diode-laser-based UV absorption results from Meyer et al. Vertical lines denote location of edge of burner. Blue dashed line is UNICORN CFD result.

As expected fit values for Φ = 1.11 in Figure 19 below continue to show now familiar trends.

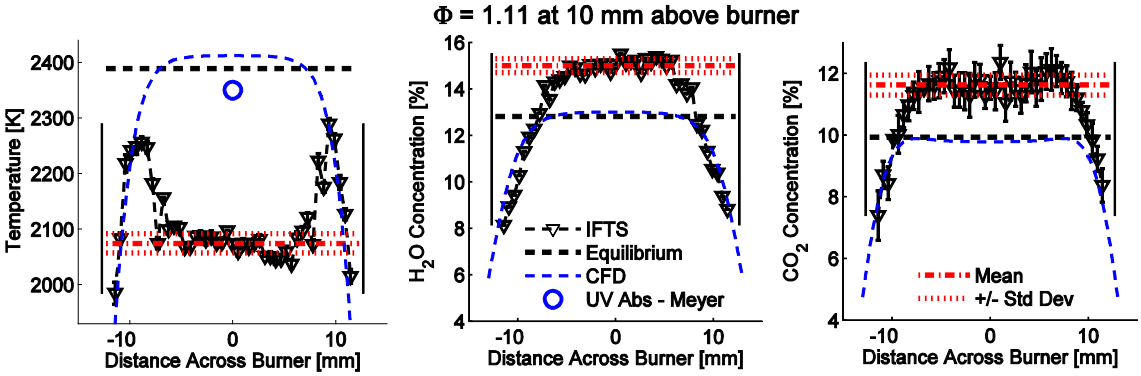

Figure 19: Temperature (left), H_2O concentration (center), and CO_2 concentration (right) for Φ = 1.11 flame at 10 mm above burner surface compared to NASA-Glenn Chemical Equilibrium Program produced values and previous diode-laser-based UV absorption results from Meyer et al. Vertical lines denote location of edge of burner. Blue dashed line is UNICORN CFD result.

Pixels with exceedingly low temperature fits also have exceedingly high H_2O concentration fits thus resulting in a consistently smooth curve when both values are multiplied together.

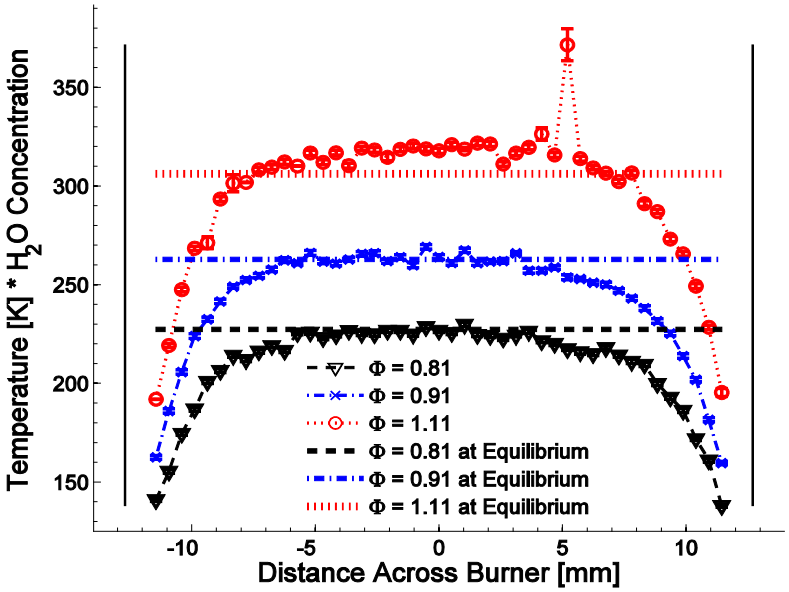

Figure 20: Product of temperature and H_2O concentration fits for three flames at 5 mm above burner surface. Horizontal lines are equilibrium values generated from NASA-Glenn CEA. Vertical lines denote location of edge of burner.

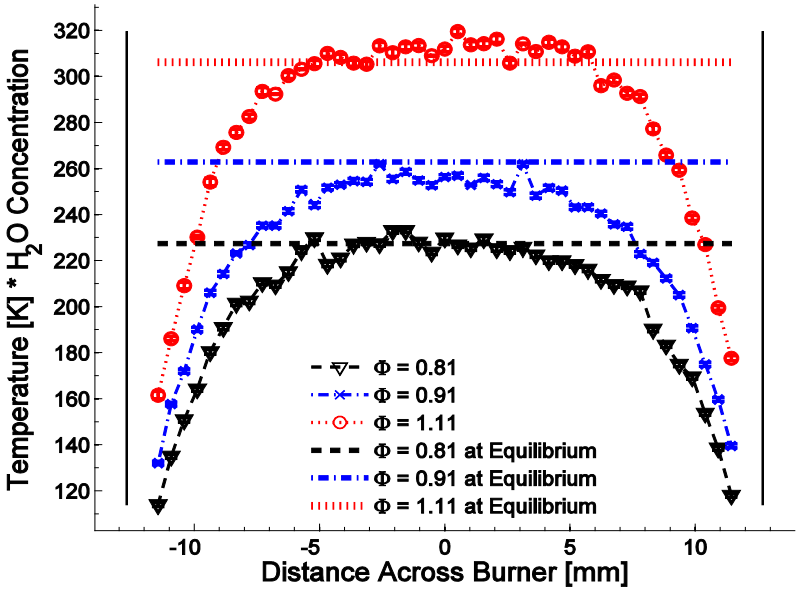

Figure 21: Product of temperature and H_2O concentration fits for three flames at 10 mm above burner surface. Horizontal lines are equilibrium values generated from NASA-Glenn CEA. Vertical lines denote location of edge of burner.

It is apparent from the previous two figures that the correct scalar values exist in the IFTS raw data collected. The problem lies in how the model is extracting this information. The current method uses a single layer model that attempts to extract both temperature and H_2O concentration simultaneously.

Temperature and Concentration Correlation

Spectrally, temperature increase raises the height of spectral line shapes across the board but the change in line peak height is not necessarily consistent from feature to feature. Increasing H_2O concentration will similarly increase line shape peak heights for H_2O spectral features but in a more consistent manner. An example of these phenomena is seen in Figure 11. In the spectral region used to fit our data the taller lines are H_2O symmetric and asymmetric stretching mode features.

Since we are varying both temperature and concentrations in our model to simultaneously match the data, it is possible for the fit to confuse temperature and concentrations. In order to show error induced as a result of this possible "mis-fit" we used a model generated ideal spectrum and fixed the fit temperature at 1% increments up to +10% and down to -10% of the ideal temperature of 2300 K. The figure below shows how the model responded by varying the concentrations in order to achieve the best fit and the resulting induced root mean squared error.

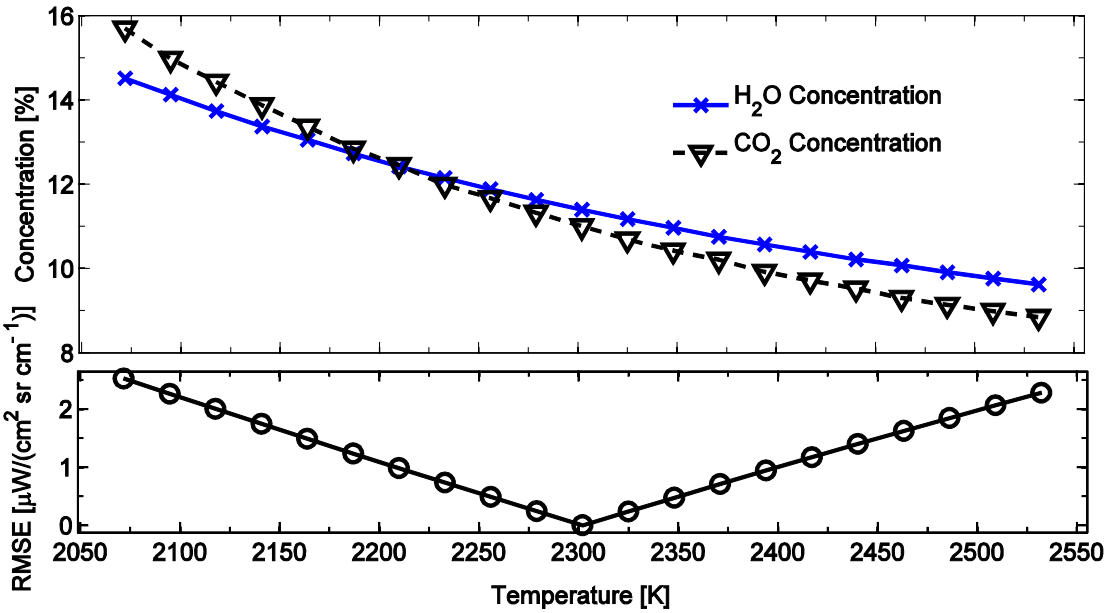

Figure 22: (above) Gas concentration fit for generated spectrum as temperature is fixed at 1% increments up to ±10% from ideal value of 2300 K. (below) Induced root mean squared error of model fit to generated spectrum. (3000 to 3400 cm^{-1} spectral window)

Figure 22 shows a 10% forced error in the temperature creates a mere 2.5 RMSE change in the overall fit. The average root mean squared error of the data fits for all three flames at pixels near the center of the flame was approximately 8 to 10 μW/(cm^2 sr cm^{-1}). Thus the fit could conceivably vary temperature and H_2O concentration a significant amount well within the noise level of the system, unable to distinguish between the two.

The above process was repeated for Figure 23 with the spectral window expanded from the calibration limited 3000 to 3400 cm^{-1} window to 3000 to 4200 cm^{-1}.

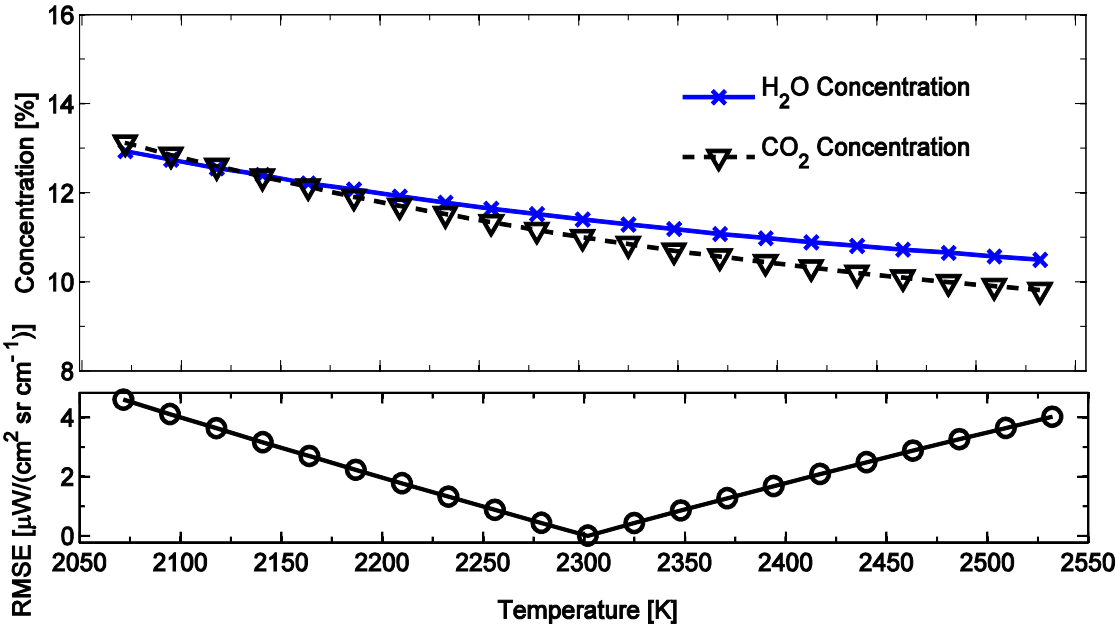

Figure 23: (above) Gas concentration fit for generated spectrum as temperature is fixed at 1% increments up to ±10% from ideal value of 2300 K. (below) Induced root mean squared error of model fit to generated spectrum. (3000 to 4200 cm^{-1} spectral window)

This spectral expansion gave the model more spectral features to work with in trying to achieve a best fit with a "locked" temperature value. As expected, the extra information resulted in less variation of H_2O and CO_2 values and an increased RMSE up to nearly 4.5 μW/(cm^2 sr cm^{-1}). Clearly the model was much better at differentiating between temperature and concentration variation when given more spectral information.

IFTS and CFD Results

UNICORN CFD results were expected to match very closely with IFTS collected data due to the maturity of the UNICORN code and its development with ties to experimental results. UNICORN calculates many flame parameters. The figure below shows just four of these parameters, averaged over 5000, 50 μs time-step iterations and

spatially mapped starting at the center of the Φ = 0.91 flame. The CFD results are symmetric about the vertical axis.

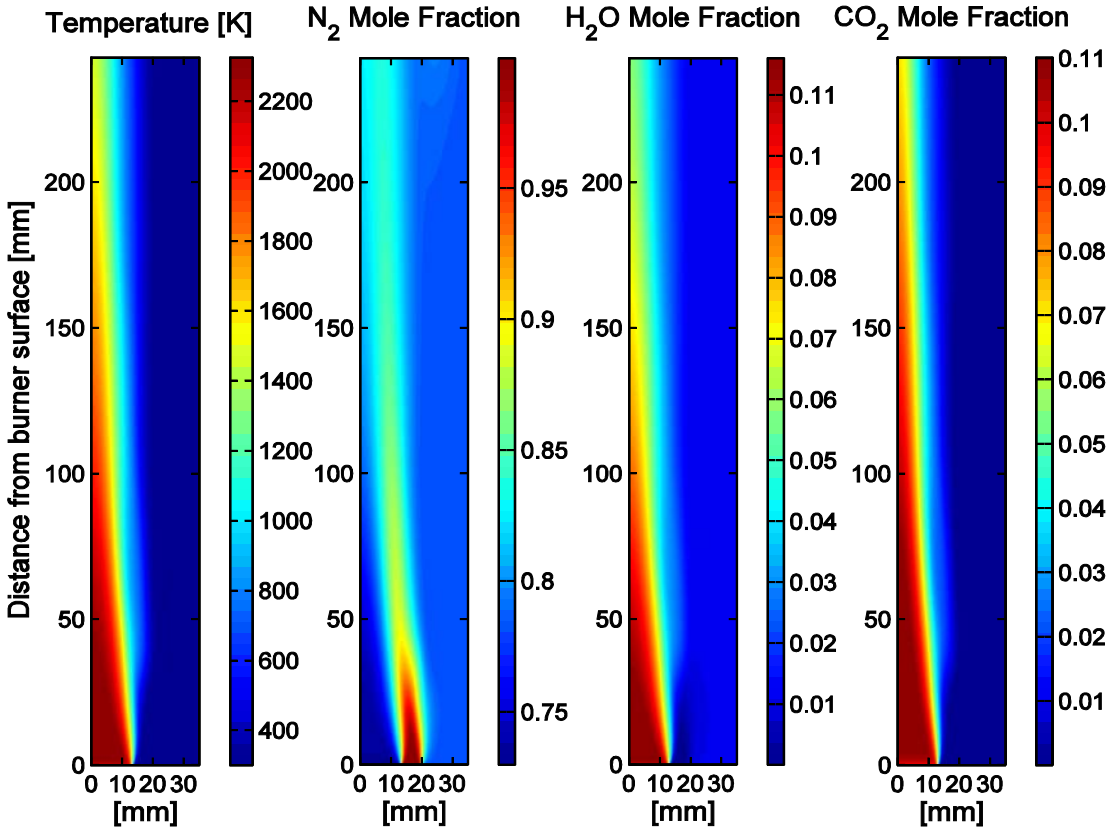

Figure 24: CFD results showing Temperature (left), N_2 mole fraction (left-center), H_2O mole fraction (right-center), and CO_2 mole fraction (right) for Φ = 0.91 simulated flame. Note N_2 co-flow (left-center) is largely mixed into the flame as soon as 40 mm above burner surface

CFD results consistently matched NASA CEA equilibrium values for each of the three flames with only temperature being modeled slightly high. There is an initial code that takes the starting mass fractions and calculates chemical reactions in order to have an initial pre-mixed gas condition for the initial flame. The second part of the process takes this initial mixture of species mass fractions and begins propagating the flame with a time step set in the UNICORN input file. This input file also contains a place to input mass

fractions of fuel, oxygen in the air, and up to three other species added to the fuel mixture. However, when simulating burning C_2H_4, UNICORN will ignore these input file variables and will rely solely on the initial mass fractions generated from the first part of the process prior to flame propagation.

Figure 25 below shows an instantaneous flame generated by UNICORN. The buoyancy effects are clearly evident and their general shapes match up with IFTS instantaneous intensity plots of Figure 9.

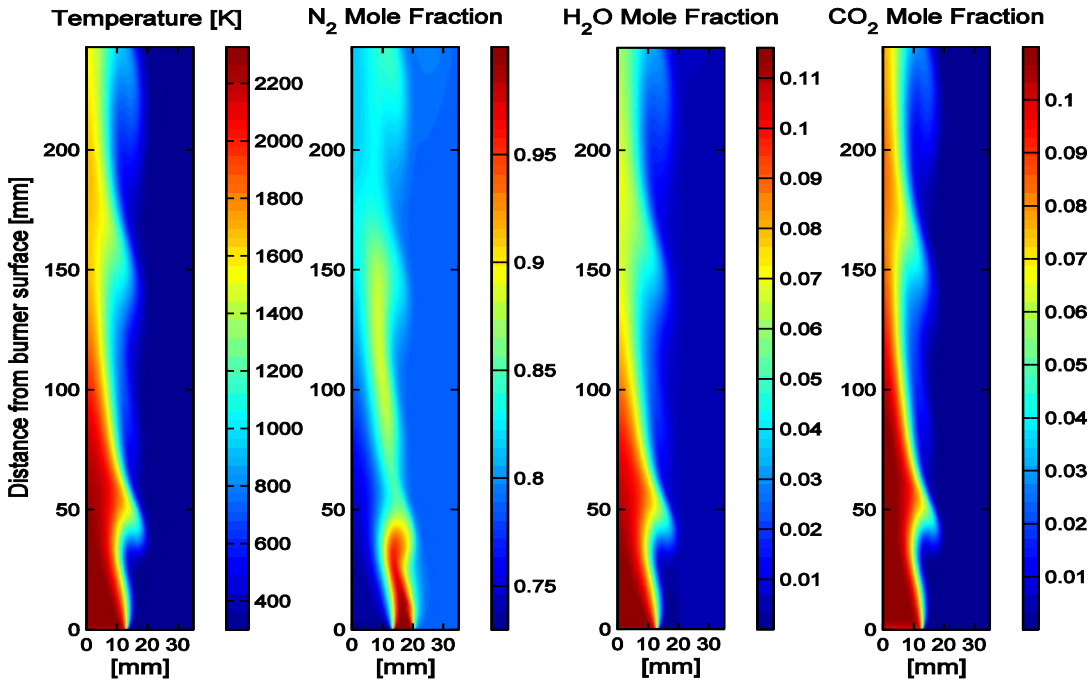

Figure 25: CFD instantaneous Φ = 0.91 flame showing temperature (left), N_2 co-flow mole fraction (left-center), H_2O mole fraction (right-center), and CO_2 mole fraction (right). Center flame temperatures and concentrations as well as vortices caused by buoyancy effects are accurately modeled.

The figures below show the now familiar IFTS fit results for this flame along with CFD derived temperature and H_2O concentration profiles at 5 mm and 10 mm above the surface of the burner.

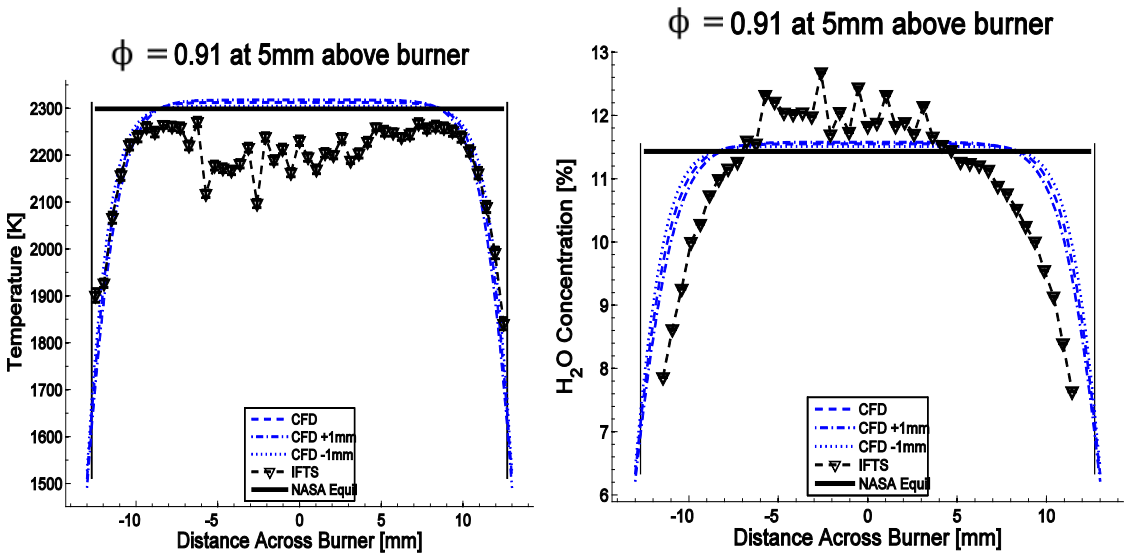

Figure 26: Temperature (left) and H_2O concentration (right) comparison of CFD and IFTS fit across the burner at 5 mm above burner surface to NASA-Glenn Chemical Equilibrium Program result. Vertical lines denote location of edge of burner. Correlation exits between pixels with low temperature and high concentration fits.

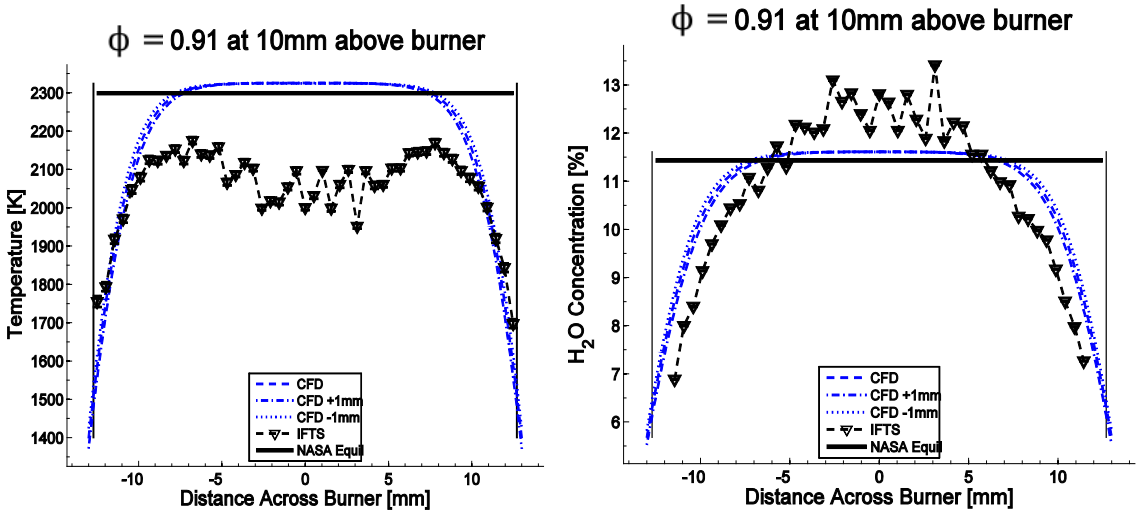

Figure 27: Temperature (left) and H_2O concentration (right) comparison of CFD and IFTS fit across the burner at 5 mm above burner surface to NASA-Glenn Chemical Equilibrium Program result. Vertical lines denote location of edge of burner. Correlation exits between pixels with low temperature and high concentration fits.

The CFD curves for temperatures and H_2O concentrations match nearly perfectly with the equilibrium values. The IFTS fits compensated for the lower temperatures seen

in left side of Figure 26 and Figure 27 with higher H_2O concentrations. Note how in this case the CFD curves for H_2O concentrations drop off later than the IFTS fit as you approach the edge of the burner.

The CFD temperature and H_2O concentration profiles are more rounded at 10 mm above the burner surface than at 5 mm. This is expected as the shape of the flame is conical in nature. This behavior is not seen as easily in the IFTS fit data due to the somewhat inconsistent nature of each pixel to pixel fit although it can be noticed in the temperature fits of Figure 26 and Figure 27.

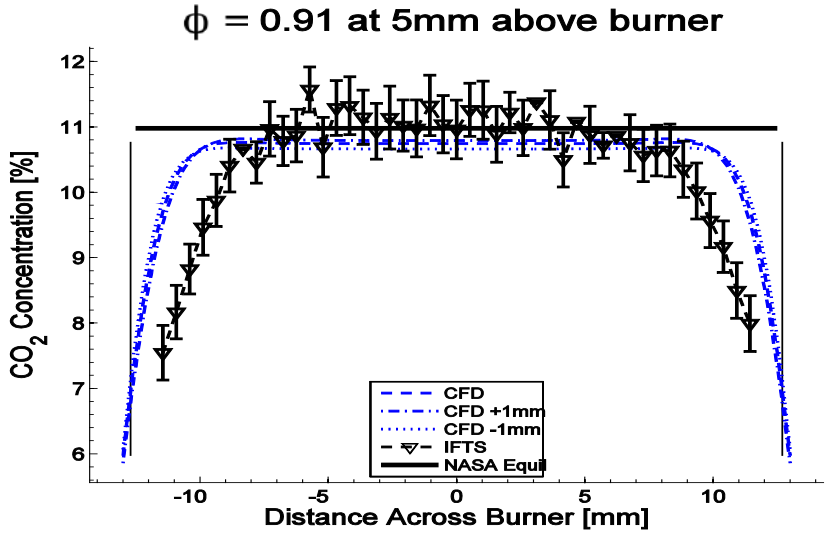

Figure 28: CO_2 concentration comparison of CFD and IFTS fit across the burner at 5 mm above burner surface to NASA-Glenn Chemical Equilibrium Program result. Vertical lines denote location of edge of burner.

Figure 28 and Figure 29 show the IFTS fit of CO_2 concentration for the $\Phi = 0.91$ flame compared to CFD and NASA CEA results. Note the model at 5 mm above the burner surface does a relatively good job in determining the correct CO_2 values in the center of the flame. Once again the fit concentrations fall off more rapidly toward the edge of the flame than the CFD model predicts.

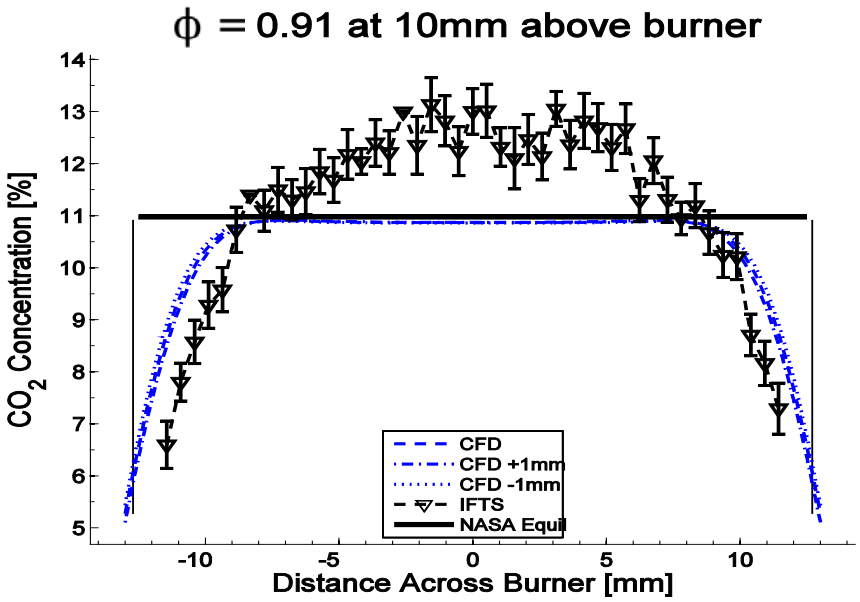

Figure 29: CO_2 concentration comparison of CFD and IFTS fit across the burner at 10 mm above burner surface to NASA-Glenn Chemical Equilibrium Program result. Vertical lines denote location of edge of burner.

Figure 28 shows excellent agreement between CFD and NASA CEA equilibrium results but the fit for CO_2 concentration is too high at 10 mm above the burner surface. This big difference in concentration fits between 5 and 10 mm above burner surface cases is not noticed in H_2O concentration fits in Figure 26 and Figure 27. Going back to Figure 22, one can see that the CO_2 concentration is also dependent on how the model fits temperature. The fit temperatures at 10 mm above the burner surface are about a hundred degrees lower than at 5 mm. This decrease is too great for a 5 mm difference in location. The reason for this lower temperature and higher CO_2 concentration at 10mm above the burner is currently not understood. While there is a similar inverse relationship between CO_2 concentration and temperature, CO_2's spectral contribution is much less than that of H_2O as seen in Figure 11. Changing CO_2 concentration should have little impact on

temperature fit results, although it is important to note the CO_2 concentration went up by almost 20% while temperature was reduced approximately 4%.

Figure 30 and Figure 31 illustrate how accurate the IFTS could be if the spectrum is calibrated more effectively and a more sophisticated model is used to fit the data, with excellent agreement between IFTS fit values, CFD, and NASA CEA. Notice the consistent behavior of the CFD producing concentration curves that drop off later than IFTS values approaching flame edge.

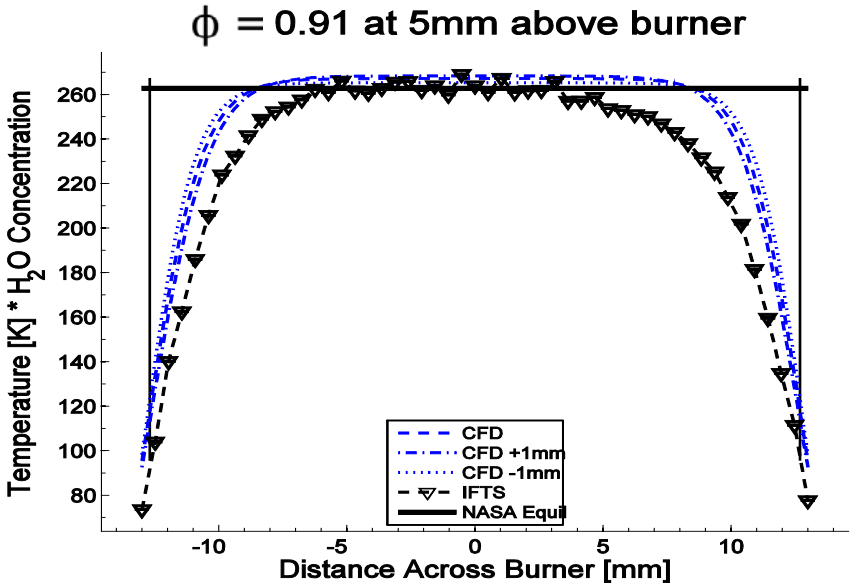

Figure 30: Temperature multiplied by H_2O concentration comparison of CFD and IFTS fit across the burner at 5 mm above burner surface to NASA-Glenn Chemical Equilibrium Program result. Vertical lines denote location of edge of burner.

Figure 31 below shows the fit results to be slightly lower than the correct value at flame center. This is due to the CO_2 concentration for this case fitting high, resulting in lower temperature fits. Since CO_2 concentration is not accounted for in Figure 31 the curve of H_2O concentration multiplied by temperature is too low.

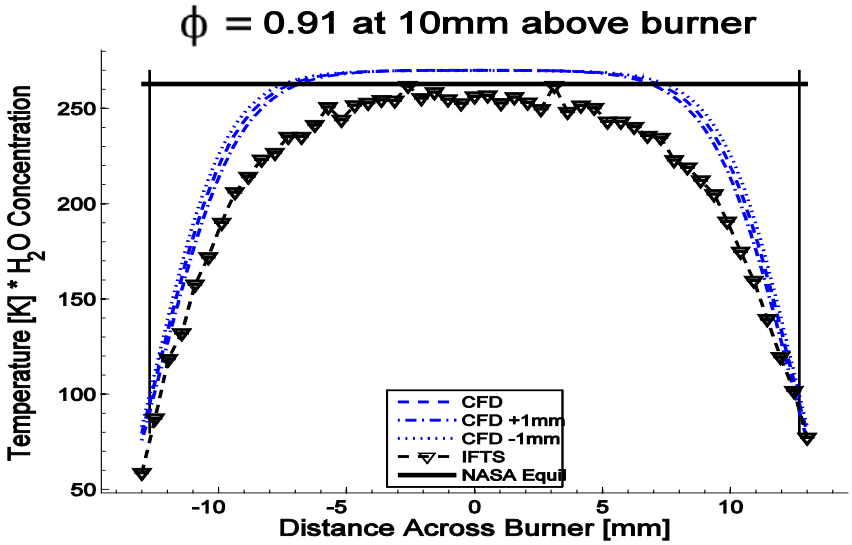

Figure 31: Temperature multiplied by H_2O concentration comparison of CFD and IFTS fit across the burner at 10 mm above burner surface to NASA-Glenn Chemical Equilibrium Program result. Vertical lines denote location of edge of burner.

Differences between CFD and IFTS Single-Layer Model Burner Representation

There are some fundamental differences between the 2-D UNICORN CFD model setup and what the IFTS actually "sees." The single-layer model used for this experiment is essentially modeling a 3-D region as a 2-D approximation. If one could build a very thin burner along a line one might expect very good agreement between IFTS fit and CFD results. However, as seen in Figure 32 below, the instrument collects light from lines of sight across the flame. In the center line of sight an overwhelming majority of photons traveling to the instrument are from the center region of the flame and dominate the recorded spectrum.

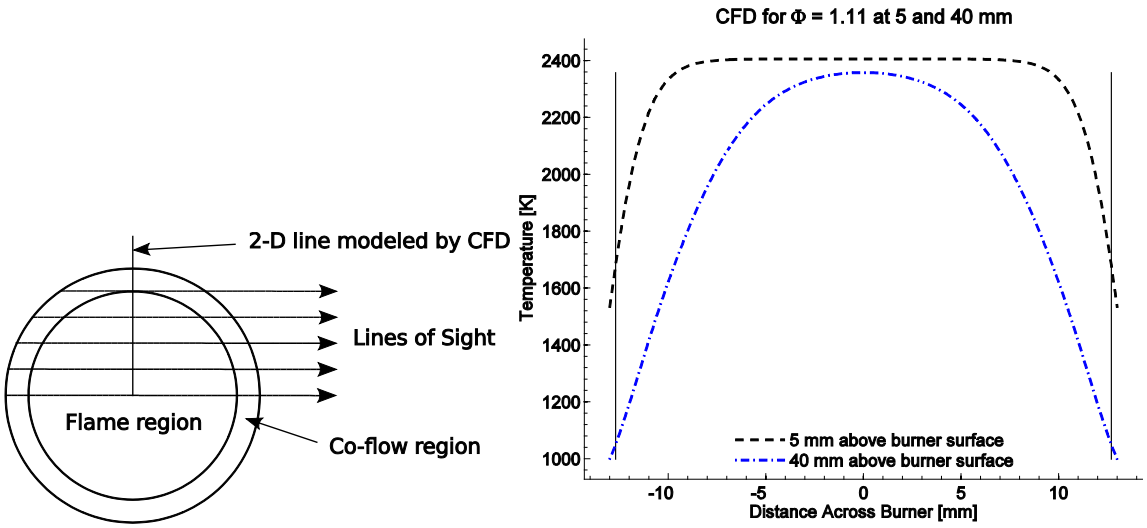

Figure 32: (left) Top view representation of how IFTS instrument "sees" flame vs. 2-D CFD approximation. (right) CFD plot of T vs radius at 5 and 40 mm above burner surface.

The lines of sight approaching the edge of the flame are largely in a mixing region of flame, co-flow, and outside air and have to travel through two of these exterior layers, one at the back of the flame and another at the front. Additionally, as we approach the edge of the flame the optical path through the flame decreases due to its cylindrical nature. As a result, entrainment of the co-flow and outside air has increased effect when compared to a 2-D representation of the flame. The right side of the figure utilizes UNICORN CFD results for the $\Phi = 1.11$ flame to demonstrate how the mixing layer can affect the temperature profile as one travels vertically up the flame.

The single layer model assumes the flame is flat and does not compensate for traveling through the outside layer. Therefore, the spectral data fit will see lower concentrations at the edge of the flame than a 2-D model can predict. This explains why IFTS concentration fit values always roll off at the edge of the flame before the predicted CFD results.

Once the H_2O concentration drops low enough the model is able to more accurately differentiate between their spectral effects and increases the temperature at the edges to a more reasonable value. This explains the temperature "spikes" present at the edge of the temperature fit results.

Further complications arise near the base of the Hencken burner simply due to its squared geometry. As the flame propagates upward it naturally becomes more cylindrical in nature but the effects of the flow field near the burner surface due to the corners are unknown.

Investigating the Single Layer Model for Flame Vertical Profile

Near the flame edge is not the only region the single layer model has difficulty. The vertical fit values seen in the figures below show a large divergence from CFD predicted values in the lower center region of the flame. In order to better represent the IFTS results, the CFD values were averaged across the horizontal axis from flame center to near the edge of the flame. This quasi-average helps account for the IFTS instrument collecting photons from a line of sight through the whole flame and the homogenous single-layer treatment used for these results.

Without this averaging technique CFD results from a vertical line at the center of the flame quickly diverge from the IFTS fit results with higher temperatures and concentrations. The divergence is primarily due to the entrainment of outside air. Traveling vertically, the outside layer of mixing fuel, co-flow, and air grows in thickness. Thus, the IFTS instrument receives more and more photons from the outside layer as you move upward. This has the effect of lowering center flame IFTS fit temperatures and

concentrations when compared to the CFD predicted center line scalar values of the flame.

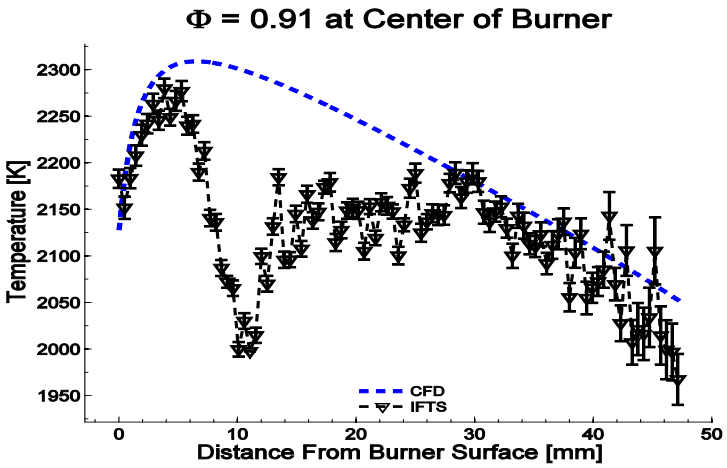

Figure 33: Φ = 0.91 flame vertical temperature fit compared to horizontally averaged CFD prediction. Drop in temperature between 5 and 12 mm above burner is consistent with horizontal fitting results.

Similar results can be seen in Figure 34 below for H_2O and CO_2 concentrations. However, instead of dipping between 5 and 12 mm the curves rise above CFD predicted results.

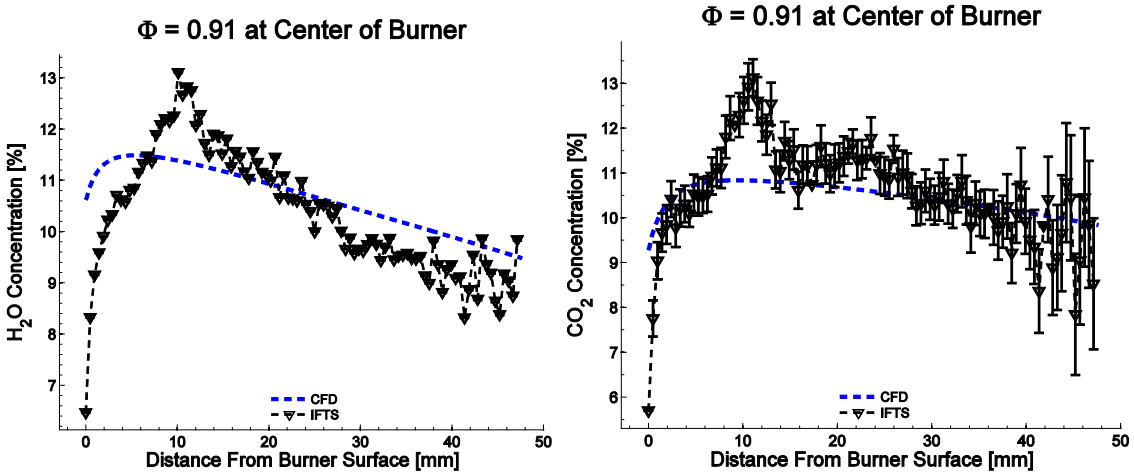

Figure 34: H_2O (left) and CO_2 concentration (right) fits for Φ = 0.91 flame compared to CFD results. Note "humps" in fit concentration curves corresponding to where temperature dips.

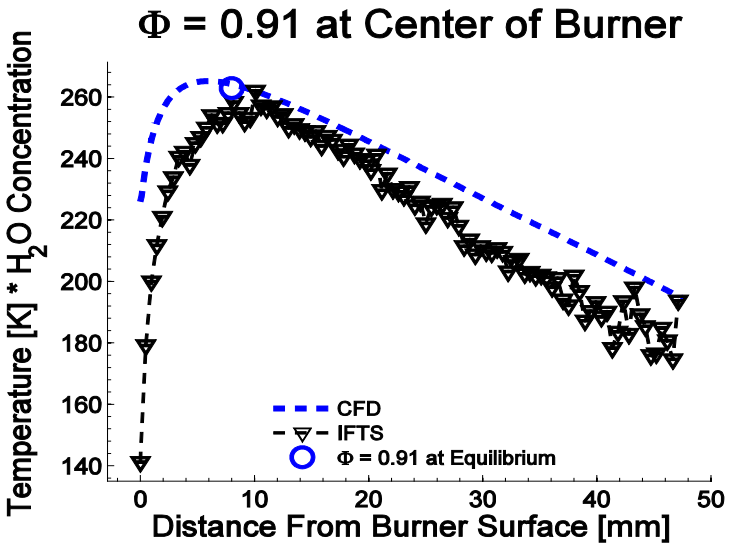

Figure 35: Temperature*H_2O concentration vertical profile of Φ = 0.91 flame compared to CFD results and NASA-Glenn CEA values.

The product of temperature and H_2O concentration in the vertical case creates a much smoother IFTS fit curve but does not quite line up with CFD results at the beginning. This could be due to the model having difficulty fitting values at the flame base due to lower signal strength or it could be a result of the CFD flame being premixed while the fuel and air exiting the Hencken burner may still be mixing at the base of the flame.

Going Vertical

In addition, as one travels vertically up the flame the signal intensity reduces with temperature and species concentrations. The signal to noise ratio degrades to a point where spectral features are indistinguishable within the noise of the system. The figure below illustrates the effects of reduced signal on the raw spectrum collected with the Telops IFTS.

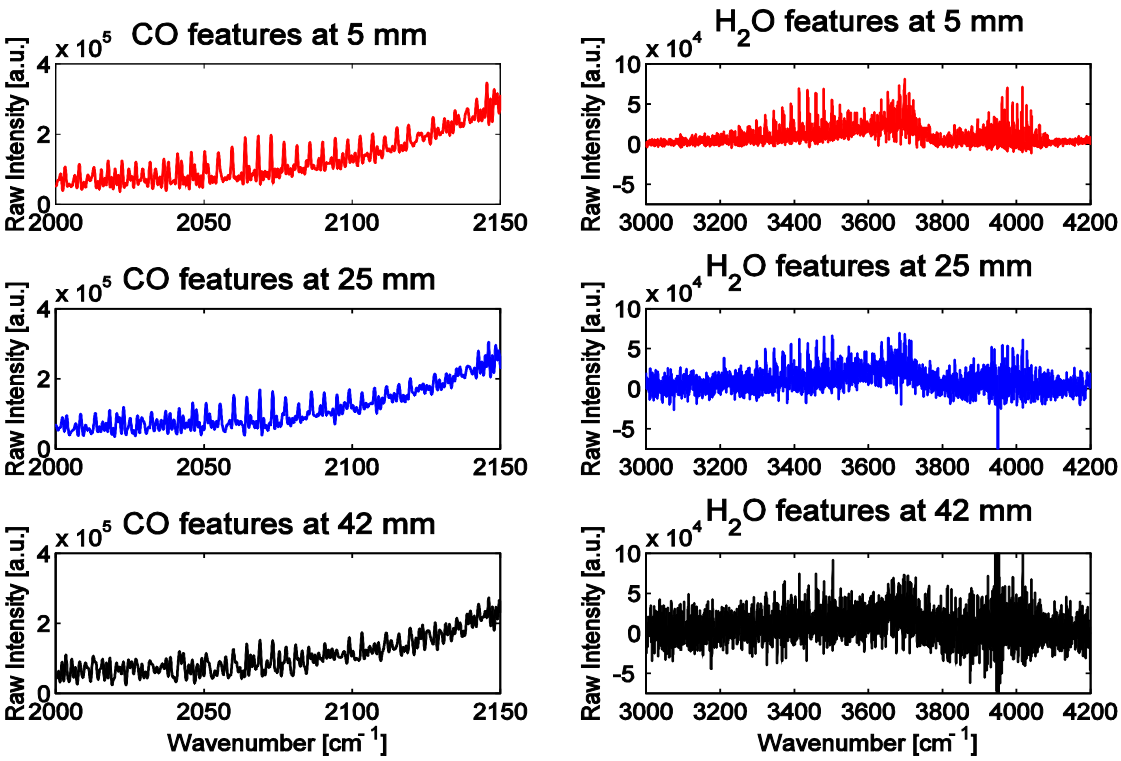

Figure 36: CO features (left) and H_2O features (right) at 5 mm (top), 25 mm (middle), and 42 mm (bottom) above burner surface.

As we move vertically one can see a progression of reduced CO concentration on the left side of the figure. This is expected as CO concentration is reduced by reacting with entrained air as the gases travel upward. The right side of the figure shows the difficulty in fitting the lower intensity regions of the flame as features of the lower spectral radiance regions of the spectrum are absorbed into the noise level of the system.

V. Conclusions

Imaging Fourier-Transform Spectrometers (IFTS) have been successfully demonstrated by Gross et al. [1,2] among others as a means to efficiently and passively recover spectroscopic data including species concentrations, temperature, and density. These parameters are useful in the study of various flow fields, to include: jet engine exhaust [1], smokestacks [2], near laminar burners [3], and turbulent flames to name a few.

This work furthers an ongoing effort to develop imaging Fourier-transform spectrometry (IFTS) for combustion diagnostics and to validate reactive-flow computational fluid dynamics (CFD) predictions. An ideal, laminar flame produced by an ethylene-fueled (C_2H_4) Hencken burner (25.4 x 25.4 mm^2 burner) with N_2 co-flow was studied using a Telops infrared IFTS featuring an Indium Antimonide (InSb), 1.5 to 5.5 μm, focal-plane array imaging the scene through a Michelson interferometer. Flames with fuel to air equivalency ratios of Φ = 0.81, 0.91, and 1.11 were imaged on a 128 x 200 pixel array with a 0.48 mm per pixel spatial resolution and 0.5 cm^{-1} spectral resolution. A single-layer radiative transfer model based on the LBLRTM code and HITRAN spectral database for high-temperature work (HITEMP) was used to simultaneously retrieve temperature (T) and concentrations of water (H_2O) and carbon dioxide (CO_2) from individual pixel spectra between 3100-3500 cm^{-1} spanning the flame at heights of 5 mm and 10 mm above the burner. CO_2 values were not determined as reliably as H_2O due to its smooth, unstructured spectral features in this window. At 5 mm height near flame center, spectrally-estimated T's were 2150, 2200, & 2125 K for

Φ = 0.81, 0.91, & 1.11 respectively, which are within 5% of previously reported experimental findings. Additionally, T & H_2O compared favorably to adiabatic flame temperatures (2175, 2300, 2385 K) and equilibrium concentrations (10.4, 11.4, 12.8 %) computed by NASA-Glenn's Chemical Equilibrium with Applications (CEA) program. UNICORN CFD predictions were in excellent agreement with CEA calculations at flame center, and predicted a fall-off in both T and H_2O with distance from flame center more slowly than the spectrally-estimated values. This is likely a shortcoming of the homogeneous assumption imposed by the single-layer model. Pixel-to-pixel variations in T and H_2O were observed which could exceed statistical fit uncertainties by a factor of 4, but the results were highly correlated. The T x H_2O product was smooth and within 3.4% of CEA calculations at flame center and compared well with CFD predictions across the entire flame. Poor signal-to-noise (SNR) in the calibration is identified as the likely cause of this systematic error. Noisy spectrums and spectral fit window limitations resulting from these calibration problems were responsible for large pixel to pixel fit variations. Developing a multi-layer model to handle flame inhomogeneities and methods to improve calibration SNR will further enhance IFTS as a valuable tool for combustion diagnostics and CFD validation.

Significance of Research

This research expanded upon previous work by Rhoby et al., highlighting how spectral window limitations and a noisy spectrum from calibration problems affect single layer model fit results. The calibration problems have since been resolved and will be presented in future work by Gross et al. This work was a vital step in advancing the

development of remote sensing combustion diagnostics tools with the ultimate goal of an efficient means to study laminar and turbulent flow fields.

Recommendations for Future Research

Development of a multi-layer model for laminar flames should allow for far more accurate fitting results at regions affected by vortices or other boundary layer effects. Using a layered approach from Equation (1) would enable the researcher to essentially peel away averaged spectra for each layer revealing the next layer's spectrum. Temperatures and species concentrations should be achievable from any location in the flame, not just the laminar base.

Appendix A – UNICORN CFD Inputs and Instruction

```
1,------CH4-Air Diffusion Flame(Global & Finite Rate Chemistry Model)-----------
2a, 2b, 0 / ISYM,IREAD,IGNIT
3a, 0, 0.01,0.0625,0.001,-40.0,0,4*0.0/ISTDY,INOISE,(X,Y,A,F of noise)
0.00,4b,4c  / RTOT,ALENG
1.0, 294.0,1.0133D+05, 1.225,1.0,10.0,0.233, 5a, 5b, 5c, 5d/ Reference Values
6a, 6b, 6c, 6d, 6e, 6f/  IFLOW,ISWIRL,ITHRM,ICHEM,IPROP,IGRAV
7a / No. of cards describing the boundaries >=4
1,2, 0.250,  0.0, 11*0.0/  J=1  Axis
9a,9b,   9c,  9d,       9e,  9f, 9g,    9h,   9i,    9j,        9k,        9l,  9m,    9n,  9o /J=1 amb N2
3,0, 0.0125, 2.0, 2.00000,0.0,0.0,300.0, 1.0,10.0, 0.058444,0.219439,0.00,0.00,0.00/J=1 FuelJet
3,0, 0.0185, 0.0, 0.25000,0.0,0.0,300.0, 1.0,10.0, 0.000000,0.000000,0.00,0.00,0.00/J=1 N2 Jet
3,0, 0.0500, 0.0, 0.01000,0.0,0.0,300.0, 1.0,10.0, 0.000000,0.233300,0.00,0.00,0.00/J=1 amb N2
4,3, 0.0500, 0.8, 11*0.0/  I=LI  Exit
0/NBODY
0/NFINJ
16a, 16b,16c,  50,0.0070, 50,0.0120, 50,0.0200, 50,0.0350, 50,0.0700, 20,0.0600/NI,I,X
3, 62,0.0248, 10,0.0050, 10,0.0090/ NJ,(J(N),Y(N))
18a, 18b, 18c, 18d, 0/  ITEND,ISECS,CFLNO,ISTORE,ISTB
1 ,  1 /  ITPRNT,IPRES
'PNT','PNT', 'PNT',  'PNT',  'PNT',  'PNT' / N-Scheme- U,V,W, H,Sp,KE
100,100, 100,  100,  100,  100 / No.of Relaxations- U,V, H,  Species
0.9,0.9, 0.99, 0.99, 0.99, 0.99/RELX-U,V,W, H,Sp,K
1.0D-08,1.0D-08, 1.0D-08, 1.0D-08, 1.0D-08, 1.0D-08/Tolerance
1000.0,1.0D+15,100000*1/Rxns.
00,2,0,0.04,0.08,0.12,0.15/IBEVOL,ISEVOL,NEVOL,(XEVOL(N),N=1,NEVOL)
0,0,6,11,26/IBDRV,NDRV,IDRV(1;10)
0,0/IBDRG,ISDRG
0,10,5,0,02.000,1000.0,01.0,1.0/NOPT,IBINJ,ITINJ,IEINJ,PDIA,PDEN,PTHR,PVEL
29a, 29b, 29c, 29d, 29e, 29f, 29e, 29f, 0,
2/IBANM,ISANM,KSYM,IPANM,X1,X2,Y1,Y2,NF,KORNT
30a, 01/NBAVE,NEAVE
'FLAME.DATA'/---- INPUT DATA -----
'FLAMEA.DATA'/---- STORE THE FINAL DATA -----
'TIME.DATA'/----- Time Evolution------
'DRIVE.DATA'/------ Driving History-----
'DRAG.DATA'/------- DRAG Data ---------
'TRACK.DATA'/------ Particle Data-------
'MOVIE.DATA'/------- Movie Data------------
'FLAVE.DATA'/------- Average Data --------
'output'/---- WRITE THE DATA -----
CCCCCCCCCCCCCCCCCCCCCCCCCCCCCCCCCCCCCCCCCCCCCCCCCCCCCC
CCCCCCCCCCCCCCCC
DRIVE-1 (Low Speed)
0,-30, 0.01,0.0625,0.001,-40.0/ISTDY,INOISE,(X,Y,A,F of noise)
   0.0,0.0,0.0,0.00,0.1,0.2,0.30,0.50,0.80,0.8/ANOISE(1-10)
   0.80, 0.80, 0.60,0.40,0.2,0.1,0.0,0.0,0.0,0.0,0.0/ANOISE(11-20)
   0.00, 0.00, 0.00,0.00,0.0,0.0,0.0,0.0,0.0,0.0,0.0/ANOISE(21-30)
```

DRIVE-2 (High Speed)
0,-30, 0.01,0.0625,0.001,-40.0/ISTDY,INOISE,(X,Y,A,F of noise)
0.0,0.0,0.0,0.00,0.1,0.2,0.40,0.80,1.20,1.2/ANOISE(1-10)
1.20, 0.90, 0.60,0.40,0.2,0.1,0.0,0.0,0.0,0.0,0.0/ANOISE(11-20)
0.00, 0.00, 0.00,0.00,0.0,0.0,0.0,0.0,0.0,0.0,0.0/ANOISE(21-30)

1000.0,1.0D+14,20*0,686*1,0,0,8*1,0,0,2*1,0,0,736*1,0,0,2000*1/Rxns.

Line 2
2a – ISYM: Leave set to 1 for symmetric flame
2b – IREAD: Reads in data from a previous simulation. Set to 0 to not read in any data. Set to 1 to read in data stored as FLAME.DATA. Set to 2 if data being read in (FLAME.DATA) has identical setup geometry including grid distribution.

Line 3 – ISTDY: Set to 1 for steady flame for initial run. Set to 0 for unsteady flame for main computational run.

Line 4
4b – RTOT: horizontal length of simulation window in meters
4c – ALENG: vertical length of simulation window in meters

Line 5
5 – Reference values used for unit-less code: Velocity U, Temperature K, Pressure Pa, Density rho, Turbulence k, Turbulence energy eps. Do NOT change
5a – Determines fuel used: 5 for ethelyne (not species numbers in UNICORN code)
5b,5c,5d – Extra species you may add to fuel. Find species number from the beginning comments of UNICORN code

Line 6
6a – IFLOW: Set to 0 for steady flow. Set to 1 for unsteady (buoyancy effects) simulation. To get the program started IFLOW was set to 0 to simplify calculations and keep UNICORN results from diverging. Results from initial run were read in to start second run with IFLOW set to 1.
6b – ISWIRL: Set to 1 if flame being modeled has swirl. (left set to 0 for this case)
6c – ITHRM: Set to 1 to include thermal effects (left set to 1)
6d – ICHEM: Set to 1 to include species transport properties (left set to 1)
6e – IPROP: Set to 1 to for non-constant transport properties (left set to 1)
6f – IGRAV: Set to 1 to include gravity effects (left set to 1). Input is multiplied by g to determine gravitational acceleration.

Line 7: Geometry and boundary setup
7a – Number of cards describing the boundaries: Sets up geometry of experiment to include locations of fuel/air mixture, ambient air regions, wall boundaries (if applicable), etc. Must be greater than or equal to 4 (one for each side of simulation window).

Lines 8 to 13 (8 to 8+7a (total number of cards)) – May add or subtract lines to change setup
8 – left as input to highlight 11*0.0 as a way to input 11 initial conditions (9e-o below) if all are zero.

9a – Boundary number: 1 – left side vertical border of simulation window, 2 – right side vertical border of simulation window, 3 – bottom horizontal border of simulation window, 4 – top horizontal border of simulation window.
9b – Type of boundary: 0 – open (no walls), 1 – wall boundary, 2 – symmetry boundary, 3 – flow exit boundary
9c – length of "card" in meters along horizontal axis: This should match RTOT or ALENG as applicable depending on the boundary.
9d – Set to 2.0 for fuel jet card and 0.8 for top horizontal exit boundary. Left set to 0 for all other cards.
9e-o – 11 initial conditions: 9e – vertical velocity in m/s; 9f - horizontal velocity in m/s; 9g – z velocity in m/s; 9h – ambient temperature in K; 9i - turbulence; 9j - turbulence energy; 9k – mass fraction of fuel; 9l – mass fraction of oxygen; 9m – mass fraction of added species 1; 9n – mass fraction of added species 2; 9o – mass fraction of added species 3

Line 16 & 17: Defines grid spacing
16a – NI (I denotes vertical axis): Defines the number of sections of equally sized grid spaces. For example, if you want the spacing to be tight in a first section and then expand to a medium spacing in a second section and finally to a large spacing in a third section you would need NI to be 3
16b – I: Number of grid spaces in the first section.
16c – X: Length of first section in meters.

For the example above the syntax for entering the grid spacing is 3, I_1,X_1, I_2,X_2, I_3,X_3 where each grouping of I,X is a section. For seven sections you would need seven of these I,X groupings.

The UNICORN Fortran code must be compiled with the correct number of grid nodes. In this experiment there are 290 defined grid spaces for NI (vertical axis). The code was compiled with LI=301 (301 grid nodes = 300 grid spaces). The code will place any remaining grid spaces (10 in this case) equally in the remaining length to the boundary.

It is recommended to use 2 iteration test runs and checking the grid spacing in the "output" file generated by UNICORN. Grid spacing should be small in regions in or near the flame and expand in ambient air regions. In the case of a wall setup, the grid spacing should compress again as you get closer to the wall. Close grid spacing provides high fidelity but will greatly increase computation time so finding a balance is key.

Line 18: Defines iterations and iteration time step
18a – ITEND: Number of iterations you wish to run. Full run requires ~15,000 to 20,000 iterations to reach "steady" flame. For initial run (6a = 0) I used 1000 iterations. The code will sometimes take about 5 minutes for the initial step to complete. It will usually speed up.
18b – ISECS: Assumed this was iteration start time, left set to zero for all runs.
18c – CFLNO: Time step for each iteration in milliseconds. I set this to 0.5 for all runs. If initial steps are very slow or the results diverge (cannot find root error) you may need to reduce this setting to 0.05 or 0.01 for 1000 steps prior to running the code again at 0.5 for 1000 (all with 6a = 0). If run diverges when changing to 6a = 1 for the final run you may need to lower the time step for another 1000 iterations to get the run started. Note whenever you

start a run and want to use results from a previous run you will need to copy FLAMEA.DATA to FLAME.DATA and set 2b = 1 or 2.

18d – ISTORE: Number of iterations per data save. Negative values will overwrite data in save files (FLAMEA.DATA and FLAVE.DATA). Positive values will keep previously saved flame data. For example, a setting of -100 will save flame data every 100 iterations and will overwrite saved data. Note using positive values can create large data files (in excess of ~3 Gb for 20,000 iterations with data saved every 200 iterations). If you require multiple instantaneous flame data you must use a positive value.

Line 29: Defines output images (.bmp)

29a – IBANM: Iteration on which to begin creating .bmp image files of simulation.

29b – ISANM: Number of iterations per image creation. Setting this to 100 will create an image every 100 iterations and is sufficient to create a movie from the resulting images.

29c – KSYM: Set to 1 for images to show full flame (duplicated along symmetric axis)

29d – IPANM: Left set to 00.

29e,f – X1,X2: Start and end x-location for image in meters (Note x-axis is vertical)

29g,h – Y1,Y2: Start and end y-location for image in meters (Note y-axis is horizontal)

Line 30: Averaged flame data setup

30a – NBAVE: Iteration on which to begin averaging instantaneous flame results in order to create averaged flame data (FLAVE.DATA)

30b – NEAVE: Iteration on which to end averaging instantaneous flame results. Set to 01 to end at 18a number.

Input File 1 for Φ = 0.81

```
1,------CH4-Air Diffusion Flame(Global & Finite Rate Chemistry Model)----------
1, 0, 0 / ISYM,IREAD,IGNIT
1, 0, 0.01,0.0625,0.001,-40.0,0,4*0.0/ISTDY,INOISE,(X,Y,A,F of noise)
0.00,0.0500,0.250  / RTOT,ALENG
1.0, 294.0,1.0133D+05, 1.225,1.0,10.0,0.233, 5, 07, 08, 09/ Reference Values
1, 0, 1, 1, 1,  1/  IFLOW,ISWIRL,ITHRM,ICHEM,IPROP,IGRAV
6  / No. of cards describing the boundaries >=4
1,2, 0.2500, 0.0, 11*0.0/  J=1  Axis
2,0, 0.2500, 0.0, 0.01000,0.0,0.0,300.0, 1.0,10.0, 0.00000,0.231371,0.006991,0.0,0.0/J=1 ambient N2
3,0, 0.0125, 2.0, 2.00000,0.0,0.0,300.0, 1.0,10.0, 0.051811,0.220928,0.000000,0.0,0.0/J=1 FuelJet
3,0, 0.0189, 0.0, 0.25000,0.0,0.0,300.0, 1.0,10.0, 0.000000,0.000000,0.000000,0.00,0.00/J=1 N2 Jet
3,0, 0.0500, 0.0, 0.01000,0.0,0.0,300.0, 1.0,10.0, 0.00000,0.231371,0.006991,0.0,0.0/J=1 ambient N2
4,3, 0.0500, 0.8, 11*0.0/  I=LI  Exit
0/NBODY
0/NFINJ
7, 20,0.002,  50,0.0070, 50,0.0120, 50,0.0200, 50,0.0350, 50,0.0700, 20,0.0600/NI,I,X
3, 62,0.0248, 10,0.0050, 10,0.0090/ NJ,(J(N),Y(N))
1000, 0,  0.50, -100, 0/  ITEND,ISECS,CFLNO,ISTORE,ISTB
1 ,  1 /  ITPRNT,IPRES
'PNT','PNT', 'PNT',  'PNT',  'PNT',  'PNT' / N-Scheme- U,V,W, H,Sp,KE
100,100, 100,  100,  100,  100 / No.of Relaxations- U,V, H,  Species
0.9,0.9, 0.99, 0.99, 0.99, 0.99/RELX-U,V,W, H,Sp,K
1.0D-08,1.0D-08, 1.0D-08, 1.0D-08, 1.0D-08, 1.0D-08/Tolerance
1000.0,1.0D+15,100000*1/Rxns.
00,2,0,0.04,0.08,0.12,0.15/IBEVOL,ISEVOL,NEVOL,(XEVOL(N),N=1,NEVOL)
0,0,6,11,26/IBDRV,NDRV,IDRV(1;10)
```

```
0,0/IBDRG,ISDRG
0,10,5,0,02.000,1000.0,01.0,1.0/NOPT,IBINJ,ITINJ,IEINJ,PDIA,PDEN,PTHR,PVEL
15000,100,1,00,0.0,0.084,0.0,0.025,0,2/IBANM,ISANM,KSYM,IPANM,X1,X2,Y1,Y2,NF,KORNT
15000,01/NBAVE,NEAVE
'FLAME.DATA'/---- INPUT DATA -----
'FLAMEA.DATA'/---- STORE THE FINAL DATA -----
'TIME.DATA'/----- Time Evolution------
'DRIVE.DATA'/------ Driving History-----
'DRAG.DATA'/------- DRAG Data ---------
'TRACK.DATA'/------ Particle Data-------
'MOVIE.DATA'/------- Movie Data------------
'FLAVE.DATA'/------- Average Data --------
'output'/---- WRITE THE DATA -----
CCCCCCCCCCCCCCCCCCCCCCCCCCCCCCCCCCCCCCCCCCCCCCCCCCCCCCCCCCCC
CCCCCCCCCC
DRIVE-1 (Low Speed)
0,-30, 0.01,0.0625,0.001,-40.0/ISTDY,INOISE,(X,Y,A,F of noise)
  0.0,0.0,0.0,0.00,0.1,0.2,0.30,0.50,0.80,0.8/ANOISE(1-10)
  0.80, 0.80, 0.60,0.40,0.2,0.1,0.0,0.0,0.0,0.0,0.0,0.0/ANOISE(11-20)
  0.00, 0.00, 0.00,0.00,0.0,0.0,0.0,0.0,0.0,0.0,0.0,0.0/ANOISE(21-30)
DRIVE-2 (High Speed)
0,-30, 0.01,0.0625,0.001,-40.0/ISTDY,INOISE,(X,Y,A,F of noise)
  0.0,0.0,0.0,0.00,0.1,0.2,0.40,0.80,1.20,1.2/ANOISE(1-10)
  1.20, 0.90, 0.60,0.40,0.2,0.1,0.0,0.0,0.0,0.0,0.0,0.0/ANOISE(11-20)
  0.00, 0.00, 0.00,0.00,0.0,0.0,0.0,0.0,0.0,0.0,0.0,0.0/ANOISE(21-30)

1000.0,1.0D+14,20*0,686*1,0,0,8*1,0,0,2*1,0,0,736*1,0,0,2000*1/Rxns.
```

Input File 2 for Φ = 0.81

```
1,------CH4-Air Diffusion Flame(Global & Finite Rate Chemistry Model)-----------
1, 2, 0 / ISYM,IREAD,IGNIT
0, 0, 0.01,0.0625,0.001,-40.0,0,4*0.0/ISTDY,INOISE,(X,Y,A,F of noise)
0.00,0.0500,0.250  / RTOT,ALENG
1.0, 294.0,1.0133D+05, 1.225,1.0,10.0,0.233, 5, 07, 08, 09/ Reference Values
1, 0, 1, 1, 1,  1/  IFLOW,ISWIRL,ITHRM,ICHEM,IPROP,IGRAV
6  / No. of cards describing the boundaries >=4
1,2, 0.2500, 0.0, 11*0.0/  J=1  Axis
2,0, 0.2500, 0.0, 0.01000,0.0,0.0,300.0, 1.0,10.0, 0.000000,0.231371,0.006991,0.00,0.00/J=1 ambient N2
3,0, 0.0125, 2.0, 2.00000,0.0,0.0,300.0, 1.0,10.0, 0.051811,0.220928,0.000000,0.00,0.00/J=1 FuelJet
3,0, 0.0189, 0.0, 0.25000,0.0,0.0,300.0, 1.0,10.0, 0.000000,0.000000,0.000000,0.00,0.00/J=1 N2 Jet
3,0, 0.0500, 0.0, 0.01000,0.0,0.0,300.0, 1.0,10.0, 0.000000,0.231371,0.006991,0.00,0.00/J=1 ambient N2
4,3, 0.0500, 0.8, 11*0.0/  I=LI  Exit
0/NBODY
0/NFINJ
7, 20,0.002,  50,0.0070, 50,0.0120, 50,0.0200, 50,0.0350, 50,0.0700, 20,0.0600/NI,I,X
3, 62,0.0248, 10,0.0050, 10,0.0090/ NJ,(J(N),Y(N))
20000, 0,  0.50, -100, 0/  ITEND,ISECS,CFLNO,ISTORE,ISTB
1 ,  1 /  ITPRNT,IPRES
'PNT','PNT', 'PNT',  'PNT',  'PNT',  'PNT' / N-Scheme- U,V,W, H,Sp,KE
100,100, 100,  100,  100,  100 / No.of Relaxations- U,V, H,  Species
0.9,0.9, 0.99, 0.99, 0.99, 0.99/RELX-U,V,W, H,Sp,K
1.0D-08,1.0D-08, 1.0D-08, 1.0D-08, 1.0D-08, 1.0D-08/Tolerance
1000.0,1.0D+15,100000*1/Rxns.
```

```
00,2,0,0.04,0.08,0.12,0.15/IBEVOL,ISEVOL,NEVOL,(XEVOL(N),N=1,NEVOL)
0,0,6,11,26/IBDRV,NDRV,IDRV(1;10)
0,0/IBDRG,ISDRG
0,10,5,0,02.000,1000.0,01.0,1.0/NOPT,IBINJ,ITINJ,IEINJ,PDIA,PDEN,PTHR,PVEL
15000,100,1,00,0.0,0.084,0.0,0.025,0,2/IBANM,ISANM,KSYM,IPANM,X1,X2,Y1,Y2,NF,KORNT
15000,01/NBAVE,NEAVE
'FLAME.DATA'/---- INPUT DATA -----
'FLAMEA.DATA'/---- STORE THE FINAL DATA -----
'TIME.DATA'/----- Time Evolution------
'DRIVE.DATA'/------ Driving History-----
'DRAG.DATA'/------- DRAG Data ---------
'TRACK.DATA'/------ Particle Data-------
'MOVIE.DATA'/------- Movie Data------------
'FLAVE.DATA'/------- Average Data --------
'output'/---- WRITE THE DATA -----
CCCCCCCCCCCCCCCCCCCCCCCCCCCCCCCCCCCCCCCCCCCCCCCCCCCCCCCCCCCCCC
CCCCCCCCCC
DRIVE-1 (Low Speed)
0,-30, 0.01,0.0625,0.001,-40.0/ISTDY,INOISE,(X,Y,A,F of noise)
   0.0,0.0,0.0,0.00,0.1,0.2,0.30,0.50,0.80,0.8/ANOISE(1-10)
   0.80, 0.80, 0.60,0.40,0.2,0.1,0.0,0.0,0.0,0.0,0.0,0.0/ANOISE(11-20)
   0.00, 0.00, 0.00,0.00,0.0,0.0,0.0,0.0,0.0,0.0,0.0,0.0/ANOISE(21-30)
DRIVE-2 (High Speed)
0,-30, 0.01,0.0625,0.001,-40.0/ISTDY,INOISE,(X,Y,A,F of noise)
   0.0,0.0,0.0,0.00,0.1,0.2,0.40,0.80,1.20,1.2/ANOISE(1-10)
   1.20, 0.90, 0.60,0.40,0.2,0.1,0.0,0.0,0.0,0.0,0.0,0.0/ANOISE(11-20)
   0.00, 0.00, 0.00,0.00,0.0,0.0,0.0,0.0,0.0,0.0,0.0,0.0/ANOISE(21-30)

1000.0,1.0D+14,20*0,686*1,0,0,8*1,0,0,2*1,0,0,736*1,0,0,2000*1/Rxns.
```

Input File 1 for Φ = 0.91

```
1,------CH4-Air Diffusion Flame(Global & Finite Rate Chemistry Model)-----------
1, 0, 0 / ISYM,IREAD,IGNIT
1, 0, 0.01,0.0625,0.001,-40.0,0,4*0.0/ISTDY,INOISE,(X,Y,A,F of noise)
0.00,0.0500,0.250  / RTOT,ALENG
1.0, 294.0,1.0133D+05, 1.225,1.0,10.0,0.233, 5, 07, 08, 09/ Reference Values
1, 0, 1, 1, 1,  1/  IFLOW,ISWIRL,ITHRM,ICHEM,IPROP,IGRAV
6  / No. of cards describing the boundaries >=4
1,2, 0.2500, 0.0, 11*0.0/  J=1  Axis
2,0, 0.2500, 0.0, 0.01000,0.0,0.0,300.0, 1.0,10.0, 0.000000,0.231371,0.006991,0.00,0.00/J=1 ambient N2
3,0, 0.0125, 2.0, 2.00000,0.0,0.0,300.0, 1.0,10.0, 0.058176,0.219445,0.000000,0.00,0.00/J=1 FuelJet
3,0, 0.0189, 0.0, 0.25000,0.0,0.0,300.0, 1.0,10.0, 0.000000,0.000000,0.000000,0.00,0.00/J=1 N2 Jet
3,0, 0.0500, 0.0, 0.01000,0.0,0.0,300.0, 1.0,10.0, 0.000000,0.231371,0.006991,0.00,0.00/J=1 ambient N2
4,3, 0.0500, 0.8, 11*0.0/  I=LI  Exit
0/NBODY
0/NFINJ
7, 20,0.002,  50,0.0070, 50,0.0120, 50,0.0200, 50,0.0350, 50,0.0700, 20,0.0600/NI,I,X
3, 62,0.0248, 10,0.0050, 10,0.0090/ NJ,(J(N),Y(N))
1000, 0,  0.50, -100, 0/  ITEND,ISECS,CFLNO,ISTORE,ISTB
1 ,  1 /  ITPRNT,IPRES
'PNT','PNT', 'PNT',  'PNT',  'PNT',  'PNT' / N-Scheme- U,V,W, H,Sp,KE
100,100, 100,  100,  100,  100 / No.of Relaxations- U,V, H,  Species
```

```
0.9,0.9, 0.99, 0.99, 0.99, 0.99/RELX-U,V,W, H,Sp,K
1.0D-08,1.0D-08, 1.0D-08, 1.0D-08, 1.0D-08, 1.0D-08/Tolerance
1000.0,1.0D+15,100000*1/Rxns.
00,2,0,0.04,0.08,0.12,0.15/IBEVOL,ISEVOL,NEVOL,(XEVOL(N),N=1,NEVOL)
0,0,6,11,26/IBDRV,NDRV,IDRV(1;10)
0,0/IBDRG,ISDRG
0,10,5,0,02.000,1000.0,01.0,1.0/NOPT,IBINJ,ITINJ,IEINJ,PDIA,PDEN,PTHR,PVEL
15000,100,1,00,0.0,0.084,0.0,0.025,0,2/IBANM,ISANM,KSYM,IPANM,X1,X2,Y1,Y2,NF,KORNT
15000,01/NBAVE,NEAVE
'FLAME.DATA'/---- INPUT DATA -----
'FLAMEA.DATA'/---- STORE THE FINAL DATA -----
'TIME.DATA'/----- Time Evolution------
'DRIVE.DATA'/------ Driving History-----
'DRAG.DATA'/------- DRAG Data ---------
'TRACK.DATA'/------ Particle Data-------
'MOVIE.DATA'/------- Movie Data------------
'FLAVE.DATA'/------- Average Data --------
'output'/---- WRITE THE DATA -----
CCCCCCCCCCCCCCCCCCCCCCCCCCCCCCCCCCCCCCCCCCCCCCCCCCCCCCCCCCCCCCCC
CCCCCCCCCC
DRIVE-1 (Low Speed)
0,-30, 0.01,0.0625,0.001,-40.0/ISTDY,INOISE,(X,Y,A,F of noise)
   0.0,0.0,0.0,0.00,0.1,0.2,0.30,0.50,0.80,0.8/ANOISE(1-10)
   0.80, 0.80, 0.60,0.40,0.2,0.1,0.0,0.0,0.0,0.0,0.0/ANOISE(11-20)
   0.00, 0.00, 0.00,0.00,0.0,0.0,0.0,0.0,0.0,0.0,0.0/ANOISE(21-30)
DRIVE-2 (High Speed)
0,-30, 0.01,0.0625,0.001,-40.0/ISTDY,INOISE,(X,Y,A,F of noise)
   0.0,0.0,0.0,0.00,0.1,0.2,0.40,0.80,1.20,1.2/ANOISE(1-10)
   1.20, 0.90, 0.60,0.40,0.2,0.1,0.0,0.0,0.0,0.0,0.0/ANOISE(11-20)
   0.00, 0.00, 0.00,0.00,0.0,0.0,0.0,0.0,0.0,0.0,0.0/ANOISE(21-30)

1000.0,1.0D+14,20*0,686*1,0,0,8*1,0,0,2*1,0,0,736*1,0,0,2000*1/Rxns.
```

Input File 2 for Φ = 0.91

```
1,------CH4-Air Diffusion Flame(Global & Finite Rate Chemistry Model)-----------
1, 2, 0 / ISYM,IREAD,IGNIT
0, 0, 0.01,0.0625,0.001,-40.0,0,4*0.0/ISTDY,INOISE,(X,Y,A,F of noise)
0.00,0.0500,0.250  / RTOT,ALENG
1.0, 294.0,1.0133D+05, 1.225,1.0,10.0,0.233, 5, 07, 08, 09/ Reference Values
1, 0, 1, 1, 1,  1/  IFLOW,ISWIRL,ITHRM,ICHEM,IPROP,IGRAV
6  / No. of cards describing the boundaries >=4
1,2, 0.2500, 0.0, 11*0.0/  J=1  Axis
2,0, 0.2500, 0.0, 0.01000,0.0,0.0,300.0, 1.0,10.0, 0.000000,0.231371,0.006991,0.00,0.00/J=1 ambient N2
3,0, 0.0125, 2.0, 2.00000,0.0,0.0,300.0, 1.0,10.0, 0.058176,0.219445,0.000000,0.00,0.00/J=1 FuelJet
3,0, 0.0189, 0.0, 0.25000,0.0,0.0,300.0, 1.0,10.0, 0.000000,0.000000,0.000000,0.00,0.00/J=1 N2 Jet
3,0, 0.0500, 0.0, 0.01000,0.0,0.0,300.0, 1.0,10.0, 0.000000,0.231371,0.006991,0.00,0.00/J=1 ambient N2
4,3, 0.0500, 0.8, 11*0.0/  I=LI  Exit
0/NBODY
0/NFINJ
7, 20,0.002,  50,0.0070, 50,0.0120, 50,0.0200, 50,0.0350, 50,0.0700, 20,0.0600/NI,I,X
3, 62,0.0248, 10,0.0050, 10,0.0090/ NJ,(J(N),Y(N))
20000, 0,  0.50, -100, 0/  ITEND,ISECS,CFLNO,ISTORE,ISTB
```

```
1 ,  1 /  ITPRNT,IPRES
'PNT','PNT', 'PNT',  'PNT',  'PNT',  'PNT' / N-Scheme- U,V,W, H,Sp,KE
100,100, 100,  100,  100,  100 / No.of Relaxations- U,V, H,  Species
0.9,0.9, 0.99, 0.99, 0.99, 0.99/RELX-U,V,W, H,Sp,K
1.0D-08,1.0D-08, 1.0D-08, 1.0D-08, 1.0D-08, 1.0D-08/Tolerance
1000.0,1.0D+15,100000*1/Rxns.
00,2,0,0.04,0.08,0.12,0.15/IBEVOL,ISEVOL,NEVOL,(XEVOL(N),N=1,NEVOL)
0,0,6,11,26/IBDRV,NDRV,IDRV(1;10)
0,0/IBDRG,ISDRG
0,10,5,0,02.000,1000.0,01.0,1.0/NOPT,IBINJ,ITINJ,IEINJ,PDIA,PDEN,PTHR,PVEL
15000,100,1,00,0.0,0.084,0.0,0.025,0,2/IBANM,ISANM,KSYM,IPANM,X1,X2,Y1,Y2,NF,KORNT
15000,01/NBAVE,NEAVE
'FLAME.DATA'/---- INPUT DATA -----
'FLAMEA.DATA'/---- STORE THE FINAL DATA -----
'TIME.DATA'/----- Time Evolution------
'DRIVE.DATA'/------ Driving History-----
'DRAG.DATA'/------- DRAG Data ---------
'TRACK.DATA'/------ Particle Data-------
'MOVIE.DATA'/------- Movie Data------------
'FLAVE.DATA'/------- Average Data --------
'output'/---- WRITE THE DATA -----
CCCCCCCCCCCCCCCCCCCCCCCCCCCCCCCCCCCCCCCCCCCCCCCCCCCCCCCCCCCCCCCC
CCCCCCCCCC
DRIVE-1 (Low Speed)
0,-30, 0.01,0.0625,0.001,-40.0/ISTDY,INOISE,(X,Y,A,F of noise)
  0.0,0.0,0.0,0.00,0.1,0.2,0.30,0.50,0.80,0.8/ANOISE(1-10)
  0.80, 0.80, 0.60,0.40,0.2,0.1,0.0,0.0,0.0,0.0,0.0/ANOISE(11-20)
  0.00, 0.00, 0.00,0.00,0.0,0.0,0.0,0.0,0.0,0.0,0.0/ANOISE(21-30)
DRIVE-2 (High Speed)
0,-30, 0.01,0.0625,0.001,-40.0/ISTDY,INOISE,(X,Y,A,F of noise)
  0.0,0.0,0.0,0.00,0.1,0.2,0.40,0.80,1.20,1.2/ANOISE(1-10)
  1.20, 0.90, 0.60,0.40,0.2,0.1,0.0,0.0,0.0,0.0,0.0/ANOISE(11-20)
  0.00, 0.00, 0.00,0.00,0.0,0.0,0.0,0.0,0.0,0.0,0.0/ANOISE(21-30)

1000.0,1.0D+14,20*0,686*1,0,0,8*1,0,0,2*1,0,0,736*1,0,0,2000*1/Rxns.
```

Input File 1 for Φ = 1.11

```
1,------CH4-Air Diffusion Flame(Global & Finite Rate Chemistry Model)-----------
1, 0, 0 / ISYM,IREAD,IGNIT
1, 0, 0.01,0.0625,0.001,-40.0,0,4*0.0/ISTDY,INOISE,(X,Y,A,F of noise)
0.00,0.0500,0.250  / RTOT,ALENG
1.0, 294.0,1.0133D+05, 1.225,1.0,10.0,0.233, 5, 07, 08, 09/ Reference Values
1, 0, 1, 1, 1,  1/  IFLOW,ISWIRL,ITHRM,ICHEM,IPROP,IGRAV
6  / No. of cards describing the boundaries >=4
1,2, 0.2500, 0.0, 11*0.0/  J=1  Axis
2,0, 0.2500, 0.0, 0.01000,0.0,0.0,300.0, 1.0,10.0, 0.000000,0.231371,0.006991,0.00,0.00/J=1 ambient N2
3,0, 0.0125, 2.0, 2.00000,0.0,0.0,300.0, 1.0,10.0, 0.069968,0.216697,0.000000,0.00,0.00/J=1 FuelJet
3,0, 0.0189, 0.0, 0.25000,0.0,0.0,300.0, 1.0,10.0, 0.000000,0.000000,0.000000,0.00,0.00/J=1 N2 Jet
3,0, 0.0500, 0.0, 0.01000,0.0,0.0,300.0, 1.0,10.0, 0.000000,0.231371,0.006991,0.00,0.00/J=1 ambient N2
4,3, 0.0500, 0.8, 11*0.0/  I=LI  Exit
0/NBODY
0/NFINJ
```

```
7, 20,0.002,  50,0.0070, 50,0.0120, 50,0.0200, 50,0.0350, 50,0.0700, 20,0.0600/NI,I,X
3, 62,0.0248, 10,0.0050, 10,0.0090/ NJ,(J(N),Y(N))
1000, 0,  0.50, -100, 0/  ITEND,ISECS,CFLNO,ISTORE,ISTB
1 ,  1 /  ITPRNT,IPRES
'PNT','PNT', 'PNT',  'PNT',  'PNT',  'PNT' / N-Scheme- U,V,W, H,Sp,KE
100,100, 100,  100,  100,  100 / No.of Relaxations- U,V, H,  Species
0.9,0.9, 0.99, 0.99, 0.99, 0.99/RELX-U,V,W, H,Sp,K
1.0D-08,1.0D-08, 1.0D-08, 1.0D-08, 1.0D-08, 1.0D-08/Tolerance
1000.0,1.0D+15,100000*1/Rxns.
00,2,0,0.04,0.08,0.12,0.15/IBEVOL,ISEVOL,NEVOL,(XEVOL(N),N=1,NEVOL)
0,0,6,11,26/IBDRV,NDRV,IDRV(1;10)
0,0/IBDRG,ISDRG
0,10,5,0,02.000,1000.0,01.0,1.0/NOPT,IBINJ,ITINJ,IEINJ,PDIA,PDEN,PTHR,PVEL
15000,100,1,00,0.0,0.084,0.0,0.025,0,2/IBANM,ISANM,KSYM,IPANM,X1,X2,Y1,Y2,NF,KORNT
15000,01/NBAVE,NEAVE
'FLAME.DATA'/---- INPUT DATA -----
'FLAMEA.DATA'/---- STORE THE FINAL DATA -----
'TIME.DATA'/----- Time Evolution------
'DRIVE.DATA'/------ Driving History-----
'DRAG.DATA'/------- DRAG Data ---------
'TRACK.DATA'/------ Particle Data-------
'MOVIE.DATA'/------- Movie Data------------
'FLAVE.DATA'/------- Average Data --------
'output'/---- WRITE THE DATA -----
CCCCCCCCCCCCCCCCCCCCCCCCCCCCCCCCCCCCCCCCCCCCCCCCCCCCCCCCCCCC
CCCCCCCCCC
DRIVE-1 (Low Speed)
0,-30, 0.01,0.0625,0.001,-40.0/ISTDY,INOISE,(X,Y,A,F of noise)
   0.0,0.0,0.0,0.00,0.1,0.2,0.30,0.50,0.80,0.8/ANOISE(1-10)
   0.80, 0.80, 0.60,0.40,0.2,0.1,0.0,0.0,0.0,0.0,0.0,0.0/ANOISE(11-20)
   0.00, 0.00, 0.00,0.00,0.0,0.0,0.0,0.0,0.0,0.0,0.0,0.0/ANOISE(21-30)
DRIVE-2 (High Speed)
0,-30, 0.01,0.0625,0.001,-40.0/ISTDY,INOISE,(X,Y,A,F of noise)
   0.0,0.0,0.0,0.00,0.1,0.2,0.40,0.80,1.20,1.2/ANOISE(1-10)
   1.20, 0.90, 0.60,0.40,0.2,0.1,0.0,0.0,0.0,0.0,0.0,0.0/ANOISE(11-20)
   0.00, 0.00, 0.00,0.00,0.0,0.0,0.0,0.0,0.0,0.0,0.0,0.0/ANOISE(21-30)

1000.0,1.0D+14,20*0,686*1,0,0,8*1,0,0,2*1,0,0,736*1,0,0,2000*1/Rxns.
```

Input File 2 for Φ = 1.11

```
1,------CH4-Air Diffusion Flame(Global & Finite Rate Chemistry Model)-----------
1, 2, 0 / ISYM,IREAD,IGNIT
0, 0, 0.01,0.0625,0.001,-40.0,0,4*0.0/ISTDY,INOISE,(X,Y,A,F of noise)
0.00,0.0500,0.250  / RTOT,ALENG
1.0, 294.0,1.0133D+05, 1.225,1.0,10.0,0.233, 5, 07, 08, 09/ Reference Values
1, 0, 1, 1, 1,  1/  IFLOW,ISWIRL,ITHRM,ICHEM,IPROP,IGRAV
6  / No. of cards describing the boundaries >=4
1,2, 0.2500, 0.0, 11*0.0/  J=1  Axis
2,0, 0.2500, 0.0, 0.01000,0.0,0.0,0.0,300.0, 1.0,10.0, 0.000000,0.231371,0.006991,0.00,0.00/J=1 ambient N2
3,0, 0.0125, 2.0, 2.00000,0.0,0.0,0.0,300.0, 1.0,10.0, 0.069968,0.216697,0.000000,0.00,0.00/J=1 FuelJet
3,0, 0.0189, 0.0, 0.25000,0.0,0.0,0.0,300.0, 1.0,10.0, 0.000000,0.000000,0.000000,0.00,0.00/J=1 N2 Jet
3,0, 0.0500, 0.0, 0.01000,0.0,0.0,0.0,300.0, 1.0,10.0, 0.000000,0.231371,0.006991,0.00,0.00/J=1 ambient N2
```

```
4,3, 0.0500, 0.8, 11*0.0/  I=LI  Exit
0/NBODY
0/NFINJ
7, 20,0.002,  50,0.0070, 50,0.0120, 50,0.0200, 50,0.0350, 50,0.0700, 20,0.0600/NI,I,X
3, 62,0.0248, 10,0.0050, 10,0.0090/ NJ,(J(N),Y(N))
20000, 0,  0.50, -100, 0/  ITEND,ISECS,CFLNO,ISTORE,ISTB
1 ,  1 /  ITPRNT,IPRES
'PNT','PNT', 'PNT',  'PNT',  'PNT',  'PNT' / N-Scheme- U,V,W, H,Sp,KE
100,100, 100,  100,  100,  100 / No.of Relaxations- U,V, H,  Species
0.9,0.9, 0.99, 0.99, 0.99, 0.99/RELX-U,V,W, H,Sp,K
1.0D-08,1.0D-08, 1.0D-08, 1.0D-08, 1.0D-08, 1.0D-08/Tolerance
1000.0,1.0D+15,100000*1/Rxns.
00,2,0,0.04,0.08,0.12,0.15/IBEVOL,ISEVOL,NEVOL,(XEVOL(N),N=1,NEVOL)
0,0,6,11,26/IBDRV,NDRV,IDRV(1;10)
0,0/IBDRG,ISDRG
0,10,5,0,02.000,1000.0,01.0,1.0/NOPT,IBINJ,ITINJ,IEINJ,PDIA,PDEN,PTHR,PVEL
15000,100,1,00,0.0,0.084,0.0,0.025,0,2/IBANM,ISANM,KSYM,IPANM,X1,X2,Y1,Y2,NF,KORNT
15000,01/NBAVE,NEAVE
'FLAME.DATA'/---- INPUT DATA -----
'FLAMEA.DATA'/---- STORE THE FINAL DATA -----
'TIME.DATA'/----- Time Evolution------
'DRIVE.DATA'/------ Driving History-----
'DRAG.DATA'/------- DRAG Data ---------
'TRACK.DATA'/------ Particle Data-------
'MOVIE.DATA'/------- Movie Data------------
'FLAVE.DATA'/------- Average Data --------
'output'/---- WRITE THE DATA -----
CCCCCCCCCCCCCCCCCCCCCCCCCCCCCCCCCCCCCCCCCCCCCCCCCCCCCCCCCCCC
CCCCCCCCCC
DRIVE-1 (Low Speed)
0,-30, 0.01,0.0625,0.001,-40.0/ISTDY,INOISE,(X,Y,A,F of noise)
   0.0,0.0,0.0,0.00,0.1,0.2,0.30,0.50,0.80,0.8/ANOISE(1-10)
   0.80, 0.80, 0.60,0.40,0.2,0.1,0.0,0.0,0.0,0.0/ANOISE(11-20)
   0.00, 0.00, 0.00,0.00,0.0,0.0,0.0,0.0,0.0,0.0/ANOISE(21-30)
DRIVE-2 (High Speed)
0,-30, 0.01,0.0625,0.001,-40.0/ISTDY,INOISE,(X,Y,A,F of noise)
   0.0,0.0,0.0,0.00,0.1,0.2,0.40,0.80,1.20,1.2/ANOISE(1-10)
   1.20, 0.90, 0.60,0.40,0.2,0.1,0.0,0.0,0.0,0.0/ANOISE(11-20)
   0.00, 0.00, 0.00,0.00,0.0,0.0,0.0,0.0,0.0,0.0/ANOISE(21-30)

1000.0,1.0D+14,20*0,686*1,0,0,8*1,0,0,2*1,0,0,736*1,0,0,2000*1/Rxns.
```

Input File Example for Setup with Wall

```
1,------CH4-Air Diffusion Flame(Global & Finite Rate Chemistry Model)-----------
1, 0, 0 / ISYM,IREAD,IGNIT
1, 0, 0.01,0.0625,0.001,-40.0,0,4*0.0/ISTDY,INOISE,(X,Y,A,F of noise)
0.00,0.3300,0.250  / RTOT,ALENG
1.0, 294.0,1.0133D+05, 1.225,1.0,10.0,0.233, 5, 07, 08, 09/ Reference Values
1, 0, 1, 1, 1,  1/  IFLOW,ISWIRL,ITHRM,ICHEM,IPROP,IGRAV
6  / No. of cards describing the boundaries >=4
1,2, 0.2500, 0.0, 11*0.0/  J=1  Axis
2,0, 0.2500, 0.0, 0.01000,0.0,0.0,300.0, 1.0,10.0, 0.000000,0.233300,0.003236,0.00,0.00/J=1 ambient N2
```

```
3,0, 0.0125, 2.0, 2.00000,0.0,0.0,300.0, 1.0,10.0, 0.058850,0.219439,0.003236,0.00,0.00/J=1 FuelJet
3,0, 0.0189, 0.0, 0.25000,0.0,0.0,300.0, 1.0,10.0, 0.000000,0.000000,0.000000,0.00,0.00/J=1 N2 Jet
3,1, 0.3300, 0.0, 0.01000,0.0,0.0,300.0, 1.0,10.0, 0.000000,0.233300,0.003236,0.00,0.00/J=1 ambient N2
4,3, 0.3300, 0.8, 11*0.0/  I=LI  Exit
0/NBODY
0/NFINJ
8, 20,0.002, 50,0.0070, 50,0.0120, 50,0.0200, 50,0.0350, 50,0.0700, 20,0.0600, 10,0.0440/NI,I,X
8, 20,0.002, 40,0.0070, 40,0.0120, 10,0.0100, 10,0.0290, 10,0.1000, 10,0.1100, 10,0.060/NJ,(J(N),Y(N))
500, 0,  0.050, -100, 0/  ITEND,ISECS,CFLNO,ISTORE,ISTB
1 ,  1 /  ITPRNT,IPRES
'PNT','PNT', 'PNT',  'PNT',  'PNT',  'PNT' / N-Scheme- U,V,W, H,Sp,KE
100,100, 100,  100,  100,  100 / No.of Relaxations- U,V, H,  Species
0.9,0.9, 0.99, 0.99, 0.99, 0.99/RELX-U,V,W, H,Sp,K
1.0D-08,1.0D-08, 1.0D-08, 1.0D-08, 1.0D-08, 1.0D-08/Tolerance
1000.0,1.0D+15,100000*1/Rxns.
00,2,0,0.04,0.08,0.12,0.15/IBEVOL,ISEVOL,NEVOL,(XEVOL(N),N=1,NEVOL)
0,0,6,11,26/IBDRV,NDRV,IDRV(1;10)
0,0/IBDRG,ISDRG
0,10,5,0,02.000,1000.0,01.0,1.0/NOPT,IBINJ,ITINJ,IEINJ,PDIA,PDEN,PTHR,PVEL
15000,50,1,00,0.0,0.084,0.0,0.025,0,2/IBANM,ISANM,KSYM,IPANM,X1,X2,Y1,Y2,NF,KORNT
15000,01/NBAVE,NEAVE
'FLAME.DATA'/---- INPUT DATA -----
'FLAMEA.DATA'/---- STORE THE FINAL DATA -----
'TIME.DATA'/----- Time Evolution------
'DRIVE.DATA'/------ Driving History-----
'DRAG.DATA'/------- DRAG Data ---------
'TRACK.DATA'/------ Particle Data-------
'MOVIE.DATA'/------- Movie Data------------
'FLAVE.DATA'/------- Average Data --------
'output'/---- WRITE THE DATA -----
CCCCCCCCCCCCCCCCCCCCCCCCCCCCCCCCCCCCCCCCCCCCCCCCCCCCCCCCCCCCCC
CCCCCCCCCC
DRIVE-1 (Low Speed)
0,-30, 0.01,0.0625,0.001,-40.0/ISTDY,INOISE,(X,Y,A,F of noise)
   0.0,0.0,0.0,0.00,0.1,0.2,0.30,0.50,0.80,0.8/ANOISE(1-10)
   0.80, 0.80, 0.60,0.40,0.2,0.1,0.0,0.0,0.0,0.0,0.0/ANOISE(11-20)
   0.00, 0.00, 0.00,0.00,0.0,0.0,0.0,0.0,0.0,0.0,0.0/ANOISE(21-30)
DRIVE-2 (High Speed)
0,-30, 0.01,0.0625,0.001,-40.0/ISTDY,INOISE,(X,Y,A,F of noise)
   0.0,0.0,0.0,0.00,0.1,0.2,0.40,0.80,1.20,1.2/ANOISE(1-10)
   1.20, 0.90, 0.60,0.40,0.2,0.1,0.0,0.0,0.0,0.0,0.0/ANOISE(11-20)
   0.00, 0.00, 0.00,0.00,0.0,0.0,0.0,0.0,0.0,0.0,0.0/ANOISE(21-30)

1000.0,1.0D+14,20*0,686*1,0,0,8*1,0,0,2*1,0,0,736*1,0,0,2000*1/Rxns.
```

Appendix B – NASA-Glenn Chemical Equilibrium with Applications Results

$\Phi = 0.81$ Flame

```
NASA-GLENN CHEMICAL EQUILIBRIUM PROGRAM CEA2, FEBRUARY 5, 2004
                  BY  BONNIE MCBRIDE AND SANFORD GORDON
 REFS: NASA RP-1311, PART I, 1994 AND NASA RP-1311, PART II, 1996

*****************************************************************

 prob case=p1112731  hp p(bar)=0.9948 1.9899
 phi=0.81
 reac
  fuel  C2H4            wt%= 100.0 t,k=  297.15
  oxid  Air             wt%= 100.0 t,k=  297.15
   output short
 output trace= 1e-5
 end

     THERMODYNAMIC EQUILIBRIUM COMBUSTION PROPERTIES AT ASSIGNED

                                PRESSURES

 CASE = p1112731

             REACTANT                      WT FRACTION      ENERGY
TEMP
                                            (SEE NOTE)     KJ/KG-MOL
K
 FUEL        C2H4                           1.0000000     52457.161
297.150
 OXIDANT     Air                            1.0000000      -154.631
297.150

 O/F=   18.25557  %FUEL=  5.193302  R,EQ.RATIO= 0.810289
PHI,EQ.RATIO= 0.810000

 THERMODYNAMIC PROPERTIES

 P, BAR           0.99480   1.9899
 T, K             2175.55  2183.70
 RHO, KG/CU M    1.5858-1 3.1622-1
 H, KJ/KG          92.049   92.049
 U, KJ/KG         -535.26  -537.23
 G, KJ/KG        -20327.5 -19967.6
 S, KJ/(KG)(K)     9.3859   9.1861

 M, (1/n)          28.835   28.853
 (dLV/dLP)t      -1.00119 -1.00092
 (dLV/dLT)p        1.0366   1.0283
 Cp, KJ/(KG)(K)    1.7651   1.6920
 GAMMAs            1.2112   1.2183
```

```
 SON VEL,M/SEC      871.7    875.6

 MOLE FRACTIONS

 *Ar             8.8388-3 8.8442-3
 *CO             2.8011-3 2.1199-3
 *CO2            1.0426-1 1.0501-1
 *H              1.1433-4 7.3399-5
 *H2             5.4029-4 4.0556-4
 H2O             1.0450-1 1.0494-1
 *NO             4.7613-3 4.8351-3
 *N2             7.3459-1 7.3500-1
 *O              4.3837-4 3.2550-4
 *OH             3.3229-3 2.8888-3
 *O2             3.5829-2 3.5560-2

  * THERMODYNAMIC PROPERTIES FITTED TO 20000.K

 NOTE. WEIGHT FRACTION OF FUEL IN TOTAL FUELS AND OF OXIDANT IN
TOTAL OXIDANTS
```

$\Phi = 0.91$ Flame

```
NASA-GLENN CHEMICAL EQUILIBRIUM PROGRAM CEA2, FEBRUARY 5, 2004
                  BY BONNIE MCBRIDE AND SANFORD GORDON
 REFS: NASA RP-1311, PART I, 1994 AND NASA RP-1311, PART II, 1996

*************************************************************
 prob case=p1112731  hp p(bar)=0.9948 1.9899
 phi=0.91
 reac
  fuel  C2H4            wt%= 100.0 t,k=  297.15
  oxid  Air             wt%= 100.0 t,k=  297.15
   output short
 output trace= 1e-5
 end

      THERMODYNAMIC EQUILIBRIUM COMBUSTION PROPERTIES AT ASSIGNED

                              PRESSURES

 CASE = p1112731

             REACTANT                     WT FRACTION      ENERGY
TEMP
                                           (SEE NOTE)     KJ/KG-MOL
K
 FUEL        C2H4                         1.0000000     52457.161
297.150
 OXIDANT     Air                          1.0000000      -154.631
297.150

 O/F=   16.24947  %FUEL=  5.797281  R,EQ.RATIO= 0.910137
PHI,EQ.RATIO= 0.910000

 THERMODYNAMIC PROPERTIES

 P, BAR           0.99480   1.9899
 T, K             2299.25  2316.62
 RHO, KG/CU M    1.4935-1 2.9689-1
 H, KJ/KG          103.38   103.38
 U, KJ/KG         -562.72  -566.87
 G, KJ/KG        -21783.2 -21483.5
 S, KJ/(KG)(K)     9.5190   9.3183

 M, (1/n)          28.701   28.738
 (dLV/dLP)t      -1.00303 -1.00250
 (dLV/dLT)p        1.0877   1.0723
 Cp, KJ/(KG)(K)    2.1954   2.0635
 GAMMAs            1.1808   1.1886
 SON VEL,M/SEC      886.8    892.6

 MOLE FRACTIONS
```

*Ar	8.7415-3	8.7530-3
*CO	9.1498-3	7.4906-3
*CO2	1.0977-1	1.1158-1
*H	3.9945-4	2.7680-4
*H2	1.7021-3	1.3674-3
H2O	1.1432-1	1.1514-1
*NO	4.5608-3	4.6279-3
*N2	7.2657-1	7.2749-1
*O	6.8829-4	5.2638-4
*OH	4.7989-3	4.2657-3
*O2	1.9296-2	1.8472-2

* THERMODYNAMIC PROPERTIES FITTED TO 20000.K

NOTE. WEIGHT FRACTION OF FUEL IN TOTAL FUELS AND OF OXIDANT IN TOTAL OXIDANTS

Φ = 1.11 Flame

```
NASA-GLENN CHEMICAL EQUILIBRIUM PROGRAM CEA2, FEBRUARY 5, 2004
                  BY BONNIE MCBRIDE AND SANFORD GORDON
 REFS: NASA RP-1311, PART I, 1994 AND NASA RP-1311, PART II, 1996

*************************************************************

 prob case=p1112731  hp p(bar)=0.9948 1.9899
 phi=1.11
 reac
  fuel  C2H4            wt%= 100.0 t,k=  297.15
  oxid  Air             wt%= 100.0 t,k=  297.15
   output short
 output trace= 1e-5
 end

    THERMODYNAMIC EQUILIBRIUM COMBUSTION PROPERTIES AT ASSIGNED

                            PRESSURES

 CASE = p1112731

             REACTANT                      WT FRACTION      ENERGY
TEMP
                                            (SEE NOTE)     KJ/KG-MOL
K
 FUEL        C2H4                           1.0000000     52457.161
297.150
 OXIDANT     Air                            1.0000000      -154.631
297.150

 O/F=   13.32163  %FUEL=  6.982444  R,EQ.RATIO= 1.109833
PHI,EQ.RATIO= 1.110000

 THERMODYNAMIC PROPERTIES

 P, BAR           0.99480   1.9899
 T, K             2388.71  2408.84
 RHO, KG/CU M    1.4081-1 2.7973-1
 H, KJ/KG          125.60   125.60
 U, KJ/KG         -580.88  -585.77
 G, KJ/KG        -23172.6 -22875.5
 S, KJ/(KG)(K)     9.7535   9.5486

 M, (1/n)          28.112   28.154
 (dLV/dLP)t      -1.00368 -1.00288
 (dLV/dLT)p        1.1033   1.0809
 Cp, KJ/(KG)(K)    2.3361   2.1485
 GAMMAs            1.1771   1.1873
 SON VEL,M/SEC      911.9    919.0
```

MOLE FRACTIONS

*Ar	8.4547-3	8.4673-3
*CO	4.0888-2	3.9453-2
*CO2	9.9344-2	1.0099-1
*H	1.4346-3	1.0874-3
*H2	8.9844-3	8.5211-3
H2O	1.2819-1	1.2939-1
*NO	1.8675-3	1.6249-3
*N2	7.0400-1	7.0518-1
*O	3.9520-4	2.6035-4
*OH	4.1035-3	3.3921-3
*O2	2.3345-3	1.6339-3

* THERMODYNAMIC PROPERTIES FITTED TO 20000.K

NOTE. WEIGHT FRACTION OF FUEL IN TOTAL FUELS AND OF OXIDANT IN TOTAL OXIDANTS

References

[1] Gross, K. C.; Tremblay, P.; and Chamberland, M. IFTS for Turbulent Flow Field Diagnostics. *Fourier Transform Spectroscopy, OSA Technical Digest (CD)* **2011**, paper FTuD1.

[2] Gross, K. C.; Bradley, K. C.; and Perram, G. P. Remote identification and quantification of industrial smokestack effluents via imaging Fourier-transform spectroscopy. *Environmental Science and Technology* **2010**, *44*, 9390-7.

[3] Rhoby, M. R.; Gross, K.C., and Blunck, D. Application of an imaging Fourier-transform spectrometer to determine two-dimensional scalar values in laminar flames. *Proceedings of the Combustion Institute* **2012**.

[4] Hancock, R. D.; Bertagnolli, K. E.; and Lucht, R. P. Nitrogen and hydrogen CARS temperature measurements in a hydrogen/air flame using a near-adiabatic flat-flame burner. *Combustion and Flame* **1997**, *109*, 323-331.

[5] Kulatilaka, W.; Lucht, R.; Hanna, S.F.; and Katta, V. Two-color, two-photon laser-induced polarization spectroscopy (LIPS) measurements of atomic hydrogen in near-adiabatic, atmospheric pressure hydrogen/air flames. *Science Direct, Combustion and Flame* **2004,** *137*, 523-537.

[6] Nguyen, QV.; and Kojima, J. Quantitative Multi-scalar Raman scattering diagnostics in high pressure flames. NASA Glenn Research Center, Propulsion Systems Division, Combustion Branch. http://www.grc.nasa.gov/WWW/combustion/zDiag.htm

[7] Wooldridge, M.S.; Torek, P.V.; Donovan, M.T.; Hall, D.L.; Miller, T.A. An Experimental Investigation of Gas-Phase Combustion Synthesis of SiO_2 Nanoparticles Using a Multi-Element Diffusion Flame Burner. *Combusion and Flame* **2002**, *131, 98-109.*

[8] Meyer, T. R.; Roy, S.; Anderson, T. N.; Miller, J. D.; Katta, V. R.; Lucht, R. P.; and Gord, J. R. Measurements of OH mole fraction and temperature up to 20 kHz by using a diode-laser-based UV absorption sensor. *Applied Optics* **2005**, *44*, 6729-6740.

[9] Roquemore, W.M.; Katta, V.R. Role of flow visualization in the development of UNICORN, *Journal of Visualization* **2000**, *Vol. 2*, 257-272.

[10] Gross, K. C.; Tremblay, P.; Bradley, K. C.; Chamberland, M.; Farley, V.; and Perram, G. P. Instrument calibration and lineshape modeling for ultraspectral imagery measurements of industrial smokestack emissions. *Proceedings of SPIE* **2010**, *7695*, 769516.

[11] Revercomb, H. E.; Buijs, H.; Howell, H. B.; Laporte, D. D.; Smith, W. L.; and Sromovsky, L. A. Radiometric calibration of IR Fourier transform spectrometers:

solution to a problem with the High-Resolution Interferometer Sounder. *Applied Optics* **1988**, *27*, 3210-3218.

[12] Clough, S. A.; Shephard, M. W.; Mlawer, E. J.; Delamere, J. S.; Iacono, M. J.; Cady-Pereira, K.; Boukabara, S.; and Brown, P. D. Atmospheric radiative transfer modeling: A summary of the AER codes. *Journal of Quantitative Spectroscopy & Radiative Transfer* **2005**, *91*, 233-244.

[13] Rothman, L. S.; Gordon, I. E.; Barbe, A.; Benner, D. C.; Bernath, P. F.; Birk, M.; Boudon, V.; Brown, L. R.; Campargue, A.; Champion, J. P.; Chance, K.; Coudert, L. H.; Dana, V.; Devi, V. M.; Fally, S.; Flaud, J. -; Gamache, R. R.; Goldman, A.; Jacquemart, D.; Kleiner, I.; Lacome, N.; Lafferty, W. J.; Mandin, J. -; Massie, S. T.; Mikhailenko, S. N.; Miller, C. E.; Moazzen-Ahmadi, N.; Naumenko, O. V.; Nikitin, A. V.; Orphal, V. I.; Perevalov, V. I.; Perrin, A.; Predoi-Cross, A.; Rinsland, C. P.; Rotger, M.; Simeckova, M.; Smith, M. A. H.; Sung, K.; Tashkun, S. A.; Tennyson, J.; Toth, R. A.; Vandaele, A. C.; and Vander Auwera, J. The HITRAN 2008 molecular spectroscopic database. *Journal of Quantitative Spectroscopy and Radiative Transfer* **2009**, *110*, 533-572.

[14] Rothman, L. S.; Gordon, I. E.; Barber, R. J.; Dothe, H.; Gamache, R. R.; Goldman, A.; Perevalov, V. I.; Tashkun, S. A.; and Tennyson, J. HITEMP, the high-temperature molecular spectroscopic database. *Journal of Quantitative Spectroscopy & Radiative Transfer* **2010**, *111*, 2139-2150.

[15] Katta, V.R.; Goss, L.P.; Roquemore, W.M. Numerical investigations of transitional H2/N2 jet diffusion flames, *AIAA Journal* **1994** *Vol. 32, 84-94.*

[16] Katta, V.R.; Roquemore, W.M. Simulation of dynamic Methane Jet Diffusion Flames Using Finite Rate Chemistry Models, *AIAA Journal* **1998** *Vol. 36, 2044-2054.*

[17] Katta, V.R.; Roquemore, W.M. Calculation of multidimensional flames using large chemical kinetics, *AIAA Journal* **2008** *Vol. 46, 1640-1650.*

[18] Blunck, D.; Basu, S.; Zheng, Y.; Katta, V.; and Gore, J. Simultaneous water vapor concentration and temperature measurements in unsteady hydrogen flames. *Proceedings of the Combustion Institute* **2009**, *32*, 2527-2534.

REPORT DOCUMENTATION PAGE

Form Approved
OMB No. 074-0188

PLEASE DO NOT RETURN YOUR FORM TO THE ABOVE ADDRESS.

1. REPORT DATE *(DD-MM-YYYY)*	2. REPORT TYPE	3. DATES COVERED *(From – To)*
21 Mar 2013	Master's Thesis	26 Aug 2011 - 21 Mar 2013

4. TITLE AND SUBTITLE

STUDY OF LAMINAR FLAME 2-D SCALAR VALUES AT VARIOUS FUEL TO AIR RATIOS USING AN IMAGING FOURIER-TRANSFORM SPECTROMETER AND 2-D CFD ANALYSIS

5a. CONTRACT NUMBER

5b. GRANT NUMBER

5c. PROGRAM ELEMENT NUMBER

6. AUTHOR(S)

Westman, Andrew J., Captain, USAF

5d. PROJECT NUMBER
N/A

5e. TASK NUMBER

5f. WORK UNIT NUMBER

7. PERFORMING ORGANIZATION NAMES(S) AND ADDRESS(S)

Air Force Institute of Technology
Graduate School of Engineering and Management (AFIT/EN)
2950 Hobson Way, Building 640
WPAFB OH 45433

8. PERFORMING ORGANIZATION REPORT NUMBER

AFIT-ENP-13-M-36

9. SPONSORING/MONITORING AGENCY NAME(S) AND ADDRESS(ES)

"Intentionally Left Blank"

10. SPONSOR/MONITOR'S ACRONYM(S)
N/A

11. SPONSOR/MONITOR'S REPORT NUMBER(S)
N/A

12. DISTRIBUTION/AVAILABILITY STATEMENT

DISTRIBUTION STATEMENT A.
APPROVED FOR PUBLIC RELEASE; DISTRIBUTION IS UNLIMITED.

13. SUPPLEMENTARY NOTES

14. ABSTRACT

This work furthers an ongoing effort to develop imaging Fourier-transform spectrometry (IFTS) for combustion diagnostics and to validate reactive-flow computational fluid dynamics (CFD) predictions. An ideal, laminar flame produced by an ethylene-fueled (C_2H_4) Hencken burner (25.4 x 25.4 mm^2 burner) with N_2 co-flow was studied using a Telops infrared IFTS featuring an Indium Antimonide (InSb), 1.5 to 5.5 μm, focal-plane array imaging the scene through a Michelson interferometer. Flame equivalency ratios of Φ = 0.81, 0.91, and 1.11 were imaged on a 128 x 200 pixel array with a 0.48 mm per pixel spatial resolution and 0.5 cm^{-1} spectral resolution. A single-layer radiative transfer model based on the Line-by-Line Radiative Transfer Model (LBLRTM) code and High Resolution Transmission (HITRAN) spectral database for high-temperature work (HITEMP) was used to simultaneously retrieve temperature (T) and concentrations of water (H_2O) and carbon dioxide (CO_2) from individual pixel spectra between 3100-3500 cm^{-1} spanning the flame at heights of 5 mm and 10 mm above the burner. CO_2 values were not determined as reliably as H_2O due to its smooth, unstructured spectral features in this window. At 5 mm height near flame center, spectrally-estimated T's were 2150, 2200, & 2125 K for Φ = 0.81, 0.91, & ...

15. SUBJECT TERMS

IFTS, combustion diagnostics, hyperspectral remote sensing, ethylene laminar flame, combustion CFD

16. SECURITY CLASSIFICATION OF:			17. LIMITATION OF ABSTRACT	18. NUMBER OF PAGES	19a. NAME OF RESPONSIBLE PERSON
a. REPORT	b. ABSTRACT	c. THIS PAGE			Assistant Professor, Kevin C. Gross, Ph.D
U	U	U	UU	83	19b. TELEPHONE NUMBER *(Include area code)* (937) 255-6565, x 4558 (kevin.gross@afit.edu)